Interaction of the hydrogen atom with laser fields: a study of relativistic effects in ionization processes

Thesis for degree of Master of Science

Ingunn Koren Rossland

Department of Physics and Technology
University of Bergen
2018

Acknowledgements

To complete such a project without good support would not have been possible. Most important I would like to express my endless gratitude to my supervisor Morten Førre for his guidance; especially for being so patient, dedicated and helpful throughout this whole project. His exceptional ability to explain and teach is a great inspiration to me.

I also want to thank Thore Espedal Moe for convincing me to apply to this master's program in the first place and also for providing helpful advice along the way. Furthermore, all the people "in the hallway", more specifically the students and faculty of the optics and atomic physics group, deserve a big thanks for always smiling and creating a positive environment. Together with all the great students and staff at the Department of Physics and Technology you have made the University feel like a second home.

I want to thank my family: my parents Ragnhild and Per Kjell and my brother Vetle for always being so supportive. Lastly, thank you to my friends and especially my boyfriend Espen for providing smiles and laughs in my everyday life.

Contents

List of Figures

Chapter 1

Introduction

Light-matter interactions have been a subject of interest for scientists and philosophers as far back as 5-400 B.C. The idea that everything must consist of elementary particles is as old as the philosopher Demokrit who lived around 460-370 BC. He named these elementary particles "atoms" which means "indivisible" [1]. When they were first discovered, atoms were believed to be the elementary building blocks of the universe, and they were named accordingly. Today we know that this is not the case, but the name remains unchanged. Considering that light-matter interactions play a crucial role in processes that make life on Earth possible and also is one of the main ways we obtain information about the world, the desire to understand these processes speaks for itself. With technological advances and the theoretical knowledge on electromagnetic radiation and quantum mechanics it is now possible to study atomic systems and processes in great detail.

The laser was invented by Theodore Maiman in 1960 [2] and has since been an important tool for experimental study of atomic systems. Brilliant x-ray laser sources called *free-electron lasers* allow us to generate coherent light at short wavelengths [3, 4, 5]. Laser technology is advancing fast, and as lasers are approaching intensities and photon energies that can accelerate electrons to relativistic velocities these effects become relevant to study. Relativistic effects have been studied theoretically in atomic systems [6, 7, 8, 9, 10] and they are the effects under study in this thesis. We will perform our study on hydrogenic systems. Hydrogenic systems are the simplest atomic systems to study, consisting of a nucleus and only one orbiting electron. In this thesis the interaction of a hydrogen atom subjected to x-ray radiation is studied, specifically looking for the effects of the relativistic corrections to the Schrödinger equation. The most important question is whether it is possible to observe any relativistic effects at all, considering that the effects are small. Another goal is to compare the ionization dynamics of the relativistic time dependent Schrödinger equation with results from other calculations and see if the Schrödinger equation is applicable in the relativistic regime. A study of the time independent Schrödinger equation with relativistic corrections has also been done in order to examine relativistic effects on photoionization cross section.

The processes under study are still complex at an atomic level which causes the need for approximations. The dipole approximation is a common approximation to apply to the electromagnetic field interacting with the atomic system, and will be used throughout this thesis. This approximation assumes the wavelength of the field to be much larger than the extension of the atomic system. By using this assumption, the spatial dependence of the field can be neglected. Furthermore, the magnetic field is neglected. It has

been shown that this approximation breaks down for high frequencies and intense fields [11, 12, 13, 14, 15, 16].

The results have been obtained by solving both the time-independent and the time-dependent Schrödinger equation numerically, modelling the interaction between the laser and the atom. A MATLAB program was written to calculate the matrix elements of the Hamiltonian to solve the time independent Schrödinger equation. All results will be shown both for a relativistic and a non-relativistic system. Time independent results include energy level calculations and plots of photoionization cross section. Afterwards, we propagate the system forward in time to study the dynamics initiated by an intense laser pulse and these results are in the form of ionization yields and probability density functions.

Useful Constants

Some constants appear frequently in atomic physics calculations, so much that it is convenient to set them to unity. In atomic units we set $\hbar = e = m_e = a_0 = 1$. When atomic units are applied the notation is shortened to a.u. The table shows an overview of the constants used in this thesis in SI-units and atomic units, including some useful conversion factors of relevant units to atomic units.

Name of constant	Unit	Symbol	Value in SI units	Value in a.u.
Speed of light	Velocity	c	$2.997\ 925 \cdot 10^{8}$ m/s	137.036 a.u.
Reduced Planck's constant	Angular momentum	$\hbar$	1.054 571 Js	1 a.u.
Mass of electron	Mass	m_e	$9.109\ 384 \cdot 10^{-31}$ kg	1 a.u.
Bohr radius for atomic hydrogen	Length	a_0	$5.291\ 772 \cdot 10^{-11}$ m	1 a.u.
Electron charge	Charge	e	$1.602\ 177 \cdot 10^{-19}$ C	1 a.u.
Permittivity in vacuum	Farads per metre	ϵ_0	$8.854\ 188 \cdot 10^{-12}$ F/m	$\epsilon_0 = \frac{1}{4\pi} = \frac{1}{\mu_0 c^2}$ a.u.
Permeability in vacuum	Newton per Ampere squared	μ_0	$1.256\ 637 \cdot 10^{-6}\,\mathrm{N/A^2}$	$\mu_0 = \frac{1}{\epsilon_0 c^2}$ a.u.
Fine structure constant	Seconds per metre	α	0.007 297 s/m	$\frac{1}{c} = \frac{1}{137.036}$ a.u.

Conversion factors

1 atomic unit of energy corresponds to:

- energy in electronvolt of 27.2114 eV
- energy in SI-units of $4.359\ 76 \cdot 10^{-18}$ J
- frequency of $6.579\ 69 \cdot 10^{15}$ Hz
- wavelength of $4.556\ 33 \cdot 10^{-8}$ m

Chapter 2

Quantum Mechanics

"Erwin with his psi can do
Calculations quite a few.
But one thing has not been seen:
Just what does psi really mean?"

- Verse about Schrödinger [17].

It is said that after a colloquium that Schrödinger held about de Broglie's thesis on the association of waves with particles and how to obtain the quantization rules, Peter Debye made a remark to Schrödinger saying that this way of thinking was childish and that to deal with waves one needs to have a wave equation. Apparently Schrödinger gave this some thought and after a few weeks at another talk he said he had found one! It was published in Annalen der Physik in 1926 under the title "Quantization as an Eigenvalue Problem". Since then, the wave function has proved to be a strong tool in quantum mechanics [17].

In this chapter an overview of important concepts in quantum mechanics will be given. This includes sections on the wave function, operators and the Schrödinger equation. The Schrödinger equation for hydrogen and its relativistic corrections will be studied in some detail. Information on these topics can be found in books on introductory quantum mechanics such as [18, 19, 20, 21].

2.1 The wave function

In classical mechanics if we want to determine the position along the x-axis of a particle at a given time; we look for the position function of time: $x(t)$. To find $x(t)$ we are using Newton's second law (or maybe the Euler-Lagrange equations) and the system's initial conditions. In quantum mechanics the state of things are quite different. If we want to determine the position of a particle we will first need the wave function $\psi(x,t)$ for the particle. To find it we must solve the Schrödinger equation. By finding the wave function $\psi(x,t)$ though, we have not determined the particle's position. The wave function is a rather curious thing. By itself it does not represent a physical observable, but if we know the wave function we can calculate the expectation value of physical observables.

Since the wave function is spread out in space for a given time t, we can only find the

probability of finding the particle at an interval $x \in [x_0, x_0 + dx]$ at time t_0:

$$|\Psi(x_0, t_0)|^2 dx \,. \tag{2.1}$$

Max Born formulated this probability representation in 1926. The particle must be somewhere so if we look for the particle along the whole x-axis,

$$\int_{-\infty}^{\infty} |\Psi(x,t)|^2 dx = 1 \,, \tag{2.2}$$

naturally, the total probability must be 1.

The wave function lives in Hilbert space. As opposed to Euclidian space with its two or three dimensions Hilbert space is an N-dimensional complex space where the rules of linear algebra and calculus are extended to be valid for a finite or infinite number of dimensions.

2.2 Operators

For every observable physical quantity in classical mechanics there is a corresponding operator in Hilbert space for quantum mechanics. There are some requirements for the operators and observables. All expectation values must be real numbers so that our operators does not give complex values for observable quantities, i.e., the expectation value of an observable must be equal to that of its complex counterpart,

$$\langle O \rangle = \langle O \rangle^*. \tag{2.3}$$

This requirement is fulfilled when our operators are hermitian which means that they fulfil the requirement:

$$\langle O \rangle = \int \Psi_1^* \hat{O} \Psi_2 dx = \int \Psi_2 (\hat{O}\Psi_1)^* dx \,. \tag{2.4}$$

The determinate states can be found by solving the eigenvalue problem

$$\hat{O}\Psi = \lambda \Psi \,. \tag{2.5}$$

If the wave function Ψ_n is an eigenfunction of the hermitian operator $\hat{O}$ then there exists a real eigenvalue λ_n to each eigenfunction. In practice this means that if we are conducting an experiment to measure a quantity O with corresponding operator $\hat{O}$ then the result of the measurement will be one of the eigenvalues λ_n.

Which observables can be measured and at what accuracy depends on the commutative properties of the operators. A commutator is defined as:

$$[\hat{O}_1, \hat{O}_2] \equiv \hat{O}_1 \hat{O}_2 - \hat{O}_2 \hat{O}_1 \,. \tag{2.6}$$

Two operators commute if $[\hat{O}_1, \hat{O}_2] = 0$. If two operators commute it means that we can determine the two observables simultaneously. An example of non-commuting operators are the position operator $\hat{x}$ and the momentum operator $\hat{p}_x = -i\hbar \frac{\partial}{\partial x}$. If we operate on a function $\psi(x)$ using the momentum operator first and then the position operator it yields one result:

$$\hat{x}\hat{p}_x\psi(x) = -i\hbar x\frac{\partial\psi(x)}{\partial x}\,. \tag{2.7}$$

Changing the order in which we operate with the two operators,

$$\hat{p}_x\hat{x}\psi(x) = -i\hbar\psi(x) - i\hbar x\frac{\partial\psi(x)}{\partial x}\,, \tag{2.8}$$

and then subtract the two results

$$(\hat{x}\hat{p}_x - \hat{p}_x\hat{x})\psi(x) = -\,i\hbar\psi(x) \tag{2.9}$$

$$\hat{x}\hat{p}_x - \hat{p}_x\hat{x} = -\,i\hbar \tag{2.10}$$

we get a non-zero commutator. Because these operators do not commute there is a restriction on the accuracy of the values of the position and the velocity. We know it from the Heisenberg's uncertainty principle,

$$\Delta x\Delta p_x \geq \frac{\hbar}{2}, \tag{2.11}$$

where Δx and Δp_x is the standard deviation for the two observables. For a general observable O the standard deviation is defined by:

$$\Delta O = \sqrt{\langle O^2\rangle - \langle O\rangle^2}\,, \tag{2.12}$$

where $\langle O^2\rangle$ is the average of the squares and $\langle O\rangle^2$ is the square of the average. Heisenberg's uncertainty principle implies that we cannot determine the values of the position and the momentum of the particle at the same time. For a plane wave that spans over all of space, $\Delta x = \infty$, the momentum (and therefore its wavelength), $\Delta p_x = 0$ can be determined. Trying to improve the accuracy of the position of the particle will result in reducing the accuracy for the momentum. More generally the uncertainty relation between two physical properties O and P is given by:

$$\Delta O\Delta P \geq \frac{1}{2}\Big|\langle[\hat{O},\hat{P}]\rangle\Big|\,. \tag{2.13}$$

If the two operators commute then $\Delta O\Delta P = 0$ and both these properties can be determined simultaneously.

2.3 The Schrödinger equation

The famous time dependent Schrödinger equation (TDSE),

$$i\hbar\frac{\partial\Psi}{\partial t} = \hat{H}\Psi\,, \tag{2.14}$$

is as fundamental as Newton's second law and it is stated as one of the postulates for quantum mechanics. It describes the changes over time for a quantum mechanical system. The Schrödinger equation can only be solved analytically for quite simple systems. Otherwise, we must solve it approximately. The $\hat{H}$ is the Hamiltonian operator. For some systems it is the sum of the kinetic and potential energy. When we are setting up the Hamiltonian we are including all interactions of the system. Below, the Hamiltonian for a particle with non-relativistic kinetic energy in one dimension exposed to a space dependent potential $V(x)$ is stated. In this case the Hamiltonian represent the total energy of the system $E_k + E_p$

$$\hat{H} = -\frac{\hbar^2}{2m}\frac{\partial^2}{\partial x^2} + V(x)\,. \tag{2.15}$$

m is the particle's mass, $\hbar$ is the reduced Planck's constant, i is the imaginary unit $i^2 = -1$ and $V(x)$ is the potential.

2.3.1 The time independent Schrödinger equation

It is useful to solve the Schrödinger equation as a stationary system as well as a time dependent one. To show that the Schrödinger equation can be separated into a solely time dependent and a space dependent part we first separate the wave function:

$$\Psi(x,t) = \psi(x)\phi(t)\,. \tag{2.16}$$

Assuming that the potential $V(x)$ is time independent is required in order to perform the separation. Then the time dependent Schrödinger equation is given by:

$$i\hbar\frac{\partial}{\partial t}\psi(x)\phi(t) = -\frac{\hbar^2}{2m}\frac{\partial^2}{\partial x^2}\psi(x)\phi(t) + V(x)\psi(x)\phi(t)\,. \tag{2.17}$$

We divide by the wavefunction on both sides and obtain:

$$i\hbar\frac{1}{\phi(t)}\frac{\partial}{\partial t}\phi(t) = -\frac{\hbar^2}{2m}\frac{1}{\psi(x)}\frac{\partial^2}{\partial x^2}\psi(x) + V(x)\,. \tag{2.18}$$

Now, the left side of the equation is only time dependent and the right side is only space dependent. For this equality to hold they must be equal to a constant. This constant will be called E. The left side of equation (2.18) is set equal to E and can be written:

$$\frac{\partial}{\partial t}\phi(t) = \frac{E}{i\hbar}\phi(t)\,. \tag{2.19}$$

The general solution for the time dependent equation is

$$\phi(t) = e^{-\frac{iE}{\hbar}t}\,. \tag{2.20}$$

The space dependent equation can be stated

$$-\frac{\hbar^2}{2m}\frac{\partial^2}{\partial x^2}\psi(x) + V(x)\psi(x) = E\psi(x) \tag{2.21}$$

and if $\hat{H} = -\frac{\hbar^2}{2m}\frac{\partial^2}{\partial x^2} + V(x)$ we can write

$$\hat{H}\psi(x) = E\psi(x)\,, \tag{2.22}$$

which is known as the time independent Schrödinger equation (TISE). The solutions to the time independent Schrödinger equation are known as stationary states.

2.3.2 The Schrödinger equation as an eigenvalue problem

Before Schrödinger's formulation of quantum mechanics Werner Heisenberg's matrix mechanics representation was already established. He published a paper on the matrix mechanics of quantum mechanics in 1925. Heisenberg's method is more suitable when solving the Schrödinger equation numerically. For this section the more convenient Dirac notation has been used. The wave function describes a certain state of a system and we

can represent it by a vector: $|\psi\rangle$. The components of the vector depend on the basis we are using. A state vector component can be written as a product of an amplitude coefficient and the corresponding basis vector component. The total vector is the sum of these. Our wave function can therefore be written as:

$$|\psi\rangle = \sum_i c_i |e_i\rangle \tag{2.23}$$

where c_i are a set of coefficients that tell you how much of $|e_i\rangle$ is contained in $|\psi\rangle$. $|c_i|^2$ is the probability of measuring the eigenvalue of $|e_i\rangle$ if the eigenfunction is orthonormalized. The particular basis $\{|e_i\rangle\}$ we are operating with is discrete. If it was continuous the sum would be replaced by an integral and it would have an infinite number of components. For obvious reasons we must restrict ourselves to discrete vectors when working numerically. Operators transform vectors and these transformations are linear:

$$\hat{O}|\psi\rangle = |\phi\rangle\,, \tag{2.24}$$

where

$$|\phi\rangle = \sum_{i=1}^{n} d_i |e_i\rangle\,. \tag{2.25}$$

We express operators as matrices where matrix elements are represented with respect to our basis,

$$O_{ji} = \langle e_j|\hat{O}|e_i\rangle\,. \tag{2.26}$$

The matrix elements show how the vector components transform from one state to another. Now, we apply this method on the time independent Schrödinger equation. To find the energy states of the system we must solve the eigenvalue problem

$$\hat{H}|\psi\rangle = E|\psi\rangle\,. \tag{2.27}$$

Inserting the expansion from equation (2.23) yields

$$\hat{H}\sum_{i=1}^{n} c_i|e_i\rangle = E\sum_{i=1}^{n} c_i|e_i\rangle\,, \tag{2.28}$$

and multiplying from the left by $\langle e_j|$ gives

$$\sum_{i=1}^{n} c_i\langle e_j|\hat{H}|e_i\rangle = E\sum_{i=1}^{n} c_i\langle e_j|e_i\rangle\,. \tag{2.29}$$

This can be written in matrix form as a system of equations where we write $\langle e_j|\hat{H}|e_i\rangle = H_{ji}$ and $\langle e_j|e_i\rangle = S_{ji}$

$$\begin{bmatrix} H_{11} & H_{12} & \dots & H_{1n} \\ H_{21} & H_{22} & \dots & H_{2n} \\ \vdots & \vdots & \ddots & \vdots \\ H_{n1} & H_{n2} & \dots & H_{n,n} \end{bmatrix} \begin{bmatrix} c_1 \\ c_2 \\ \vdots \\ c_n \end{bmatrix} = E \begin{bmatrix} S_{11} & S_{12} & \dots & S_{1n} \\ S_{21} & S_{22} & \dots & S_{2n} \\ \vdots & \vdots & \ddots & \vdots \\ S_{n1} & S_{n2} & \dots & S_{n,n} \end{bmatrix} \begin{bmatrix} c_1 \\ c_2 \\ \vdots \\ c_n \end{bmatrix} \tag{2.30}$$

In shorter notation:

$$H\mathbf{c} = ES\mathbf{c}\,. \tag{2.31}$$

The matrix S is called the overlap matrix and is necessary when the basis functions are not orthogonal. If they were orthogonal then $S = I_n$.

2.4 Hydrogen

Hydrogen, the simplest of elements and also the most common element in the universe, is the element under study in this section. In its most common form the hydrogen atom consists of only a positively charged proton with an orbiting negatively charged electron. The proton has a mass much larger than the electron and is assumed located at the origin; the center of mass. As such, the proton is assumed to be stationary while the electron is orbiting it. This section will describe the Schrödinger equation for a field-free hydrogen atom. The relativistic corrections to the field-free Schrödinger equation will be described, the so-called fine structure.

2.4.1 Separation of variables

A system like the hydrogen atom is best described using spherical coordinates. The electron is moving in a Coulomb potential, $V(r)$, because of the positively charged proton. Apart from this we do not take into account the properties of the proton. The time independent Schrödinger equation can be written:

$$-\frac{\hbar^2}{2m}\nabla^2\Psi(\mathbf{r}) + V(r)\Psi(\mathbf{r}) = E\Psi(\mathbf{r})\,, \tag{2.32}$$

where m is the mass of the electron and the momentum is $\hat{p} = -i\hbar\nabla$. The Laplacian operator ∇^2 in spherical coordinates is given by:

$$\nabla^2 = \frac{1}{r^2}\frac{\partial}{\partial r}\left(r^2\frac{\partial}{\partial r}\right) + \frac{1}{r^2}\left[\frac{1}{\sin\theta}\frac{\partial}{\partial\theta}\left(\sin\theta\frac{\partial}{\partial\theta}\right) + \frac{1}{\sin^2\theta}\left(\frac{\partial^2}{\partial\phi^2}\right)\right]. \tag{2.33}$$

The wave function $\Psi(\mathbf{r})$ can be separated into a product of a radial part and an angular part:

$$\Psi(\mathbf{r}) = R(r)Y_{lm}(\theta,\phi)\,. \tag{2.34}$$

The part inside the square brackets in equation (2.33) can be recognized as the operator

$$\hat{L}^2 = -\hbar^2\left[\frac{1}{\sin\theta}\frac{\partial}{\partial\theta}\left(\sin\theta\frac{\partial}{\partial\theta}\right) + \frac{1}{\sin^2\theta}\left(\frac{\partial^2}{\partial\phi^2}\right)\right] \tag{2.35}$$

which is the orbital angular momentum squared. The angular momentum operator is given from classical mechanics: $\hat{L} = \hat{r}\times\hat{p} = \hat{r}\times -i\hbar\nabla$. The expression for the wave function (2.34) is substituted into (2.32) and then divided by the wave function. In addition we write the expression in the square brackets of (2.33) as $-\frac{\hat{L}^2}{\hbar^2}$ and get the following Schrödinger equation:

$$-\frac{\hbar^2}{2mr^2}\frac{1}{R(r)}\frac{\partial}{\partial r}\left(r^2\frac{\partial R(r)}{\partial r}\right) + V(r) + \frac{1}{Y_{lm}(\theta,\phi)}\frac{\hat{L}^2}{2\hbar^2mr^2}Y_{lm}(\theta,\phi) = E\,. \tag{2.36}$$

The operator $\hat{L}^2$ commutes with all the individual components of the angular momentum $\hat{L}$: $\hat{L}_x$, $\hat{L}_y$ and $\hat{L}_z$, but the individual components does not commute with each other. We shall therefore consider only the eigenvalues of the operator $\hat{L}_z$:

$$\hat{L}_z = -i\hbar \frac{\partial}{\partial \phi} \,. \tag{2.37}$$

Only the third term of the equation (2.36) describes the angular part of the Schrödinger equation. The operators $\hat{L}^2$ and $\hat{L}_z$ has known eigenfunctions:

$$\hat{L}^2 Y_{lm}(\theta, \phi) = \hbar^2 l(l+1) Y_{lm}(\theta, \phi) \tag{2.38}$$

$$\hat{L}_z Y_{lm}(\theta, \phi) = \hbar m Y_{lm}(\theta, \phi) \,. \tag{2.39}$$

The eigenfunctions $Y_{lm}(\theta, \phi)$ are called spherical harmonics and they are eigenfunctions of both operators $\hat{L}^2$ and $\hat{L}_z$. Because of the nature of the solutions l must take non-negative integer values and for each l there are $(2l+1)$ possible values for m. The integers l and m in the eigenvalues are called the orbital angular momentum quantum number and the magnetic quantum number, respectively, and they can take the values stated below:

$$l = 0, 1, 2, 3... \tag{2.40}$$

$$m = -l, -l+1, ..., -1, 0, 1, ..., l-1, l \,. \tag{2.41}$$

Now that the solutions for the angular equation are obtained, reducing the radial wave function is convenient,

$$\mathcal{U}(r) \equiv rR(r) \,. \tag{2.42}$$

Since the eigenvalues of the angular part is known, the eigenvalues can be inserted in (2.36) and the so-called radial equation is acquired:

$$-\frac{\hbar^2}{2m}\frac{d^2\mathcal{U}(r)}{dr^2} + \left[V(r) + \frac{\hbar^2}{2m}\frac{l(l+1)}{r^2}\right]\mathcal{U}(r) = E\,\mathcal{U}(r) \,. \tag{2.43}$$

Solving the radial equation gives the famous Bohr formula for the allowed energy values of the hydrogen atom,

$$E_n = -\frac{1}{n^2}\left(\frac{m}{2\hbar^2}\left(\frac{e^2}{4\pi\epsilon_0}\right)^2\right) = \frac{E_1}{n^2} \,, \tag{2.44}$$

where n is the principal quantum number and ϵ_0 is the vacuum permittivity. E_1 is the energy of the electron in the ground state; also called the binding energy because it is the amount of energy needed to ionize the atom from the ground state,

$$E_1 \simeq 13.6\,\text{eV} \,. \tag{2.45}$$

2.4.2 The fine structure of hydrogen

Based on the non-relativistic Schrödinger equation (2.32) for hydrogen the Hamiltonian can be written as:

$$\hat{H}_0 = \frac{\hat{p}^2}{2m} + V(r)\,. \tag{2.46}$$

Still, there are effects in the atomic system that we have not accounted for. These are the relativistic effects and they can be implemented as correction terms to our Hamiltonian. First of these are the correction to the kinetic energy, coming from special relativity as the electron reaches speeds comparable to the speed of light. The second is the spin-orbit coupling arising from the fact that the electron's and proton's charges are the sources of magnetic fields. The last correction is the Darwin term, only occurring when the spin-orbit coupling is not present i.e., $l = 0$ states.

The corrections we are dealing with in this chapter can be found to be of order

$$\alpha^2 = \frac{1}{(c)^2} \simeq \frac{1}{137^2} \tag{2.47}$$

in atomic units. These additional terms have the effect that they are splitting the energy levels further and they give the hydrogen energy spectrum a fine structure, this is why they have been named *the fine structure*. The constant α is appearing in all the corrections and for this reason it has been named the *fine structure constant*. Even though we are getting a much more complex and correct result adding these terms, there are still effects that we have not taken into account. These are the Lamb shift and the hyperfine structure. These corrections are of order 1000 smaller than our relativistic corrections and we choose to ignore them here.

Correction to the Kinetic Energy

The first relativistic correction term can be found by studying Einstein's famous equation

$$E = \sqrt{p^2c^2 + m^2c^4} \tag{2.48}$$

for the total energy of a free particle where p is the momentum and m is the rest mass. The relativistic expression for the kinetic energy is found by subtracting the rest mass energy:

$$E_k = \sqrt{p^2c^2 + m^2c^4} - mc^2\,. \tag{2.49}$$

As p becomes an operator in quantum mechanics the square root expression is inconvenient for numerical approximation. Therefore, we want to make an expansion. First, taking mc^2 out of the root,

$$E_k = mc^2\sqrt{1 + \frac{p^2}{mc^2}} - mc^2\,, \tag{2.50}$$

and then applying the binomial theorem to expand the root yields:

$$E_k = mc^2\left(1 + \frac{p^2}{2m^2c^2} - \frac{p^4}{8m^4c^4} + \frac{p^6}{16m^6c^6} - \ ...\right) - mc^2\,. \tag{2.51}$$

.

The first and last term cancels.

$$E_k = \frac{p^2}{2m} - \frac{p^4}{8m^3c^2} + \frac{p^6}{16m^5c^4} - ... \tag{2.52}$$

We shall only include the first order correction, i.e. the term $\propto p^4$. As can be seen the third term is proportional to α^4 and is neglected here. Our Hamiltonian (2.46) gets the correction term:

$$\hat{H}_1 = -\frac{\hat{p}^4}{8m^3c^2}\,. \tag{2.53}$$

From first order perturbation theory the correction of the energy levels due to this correction term is given by [21],

$$\Delta E_1 = |E_n|\frac{\alpha^2}{n}\left(\frac{1}{l+\frac{1}{2}} - \frac{3}{4n}\right)\,. \tag{2.54}$$

E_n is given by the Bohr formula, see equation (2.44). l is the orbital angular momentum quantum number, which partly lifts the degeneracy of the energy levels.

Spin-orbit Coupling

From the reference frame of the electron the nucleus is orbiting it. The positive charge moving in a loop creates a magnetic field that exerts a torque on the electron. The energy associated with the torque is given by the Hamiltonian:

$$\hat{H}_2 = -\boldsymbol{\mu}\cdot\mathbf{B}\,. \tag{2.55}$$

$\boldsymbol{\mu}$ is the dipole moment of the electron and $\mathbf{B}$ is the magnetic field of the proton. The magnetic field arises because the orbiting proton creates a current. The relationship between the two can be found using Biot-Savart's law [22]:

$$\mathbf{B} = \frac{\mu_0 I}{4\pi}\int\frac{d\mathbf{l}'\times\hat{\mathbf{r}}}{r^2} = \frac{\mu_0 I}{2r}\,. \tag{2.56}$$

The integral gives $2\pi r$ when a circular orbit of radius r has been assumed. I is the current and μ_0 is the permeability of free space. A charge e is orbiting with a certain period T and the current can be stated $I = \frac{e}{T}$. Returning to the proton's frame of reference, the electron has orbital angular momentum that can be expressed using the orbiting period:

$$L = mvr = \frac{2\pi mr^2}{T} \qquad \rightarrow \qquad I = \frac{eL}{2\pi mr^2}\,, \tag{2.57}$$

where m is the mass of the electron. Both $\mathbf{B}$ and $\mathbf{L}$ are pointing in the same direction and we can write the magnetic field using the new expression for the current,

$$\mathbf{B} = \frac{\mu_0 e}{4\pi mr^3}\mathbf{L}\,, \tag{2.58}$$

replacing μ_0 with $\frac{1}{\epsilon_0 c^2}$ gives:

$$\mathbf{B} = \frac{1}{4\pi\epsilon_0}\frac{e}{mc^2r^3}\mathbf{L}\,. \tag{2.59}$$

The magnetic dipole moment created by a current loop is defined as:

$$\boldsymbol{\mu} \equiv I\mathbf{a}\,, \tag{2.60}$$

where $\mathbf{a}$ is the vector area of the loop being $\mathbf{a} = \pi r^2$ for an electron orbiting in a plane and I is the current. The current being $I = \frac{e}{T}$ as before yields:

$$\boldsymbol{\mu} = \frac{e\pi r^2}{T}\,. \tag{2.61}$$

If we now consider the spin orbital angular momentum of the electron

$$\mathbf{S} = \mathbf{r} \times \mathbf{p} = \frac{2\pi m r^2}{T} \qquad \rightarrow \qquad T = \frac{2\pi m r^2}{S}\,. \tag{2.62}$$

Replacing T in (2.61) with the right hand expression in (2.62) yields:

$$\boldsymbol{\mu} = -\frac{e}{2m}\mathbf{S}\,. \tag{2.63}$$

The electron magnetic moment is twice the classical value of the magnetic moment of a spherical object with charge e. This factor cancels out with a kinematic correction known as the Thomas precession [19]. Inserting the results from (2.59) and (2.63) into (2.55) gives the term called the *spin-orbit coupling*:

$$\hat{H}_2 = \frac{e^2}{8\pi\epsilon_0}\frac{1}{m^2c^2r^3}\hat{\mathbf{L}}\cdot\hat{\mathbf{S}}\,. \tag{2.64}$$

The Hamiltonian (2.46) does not commute with the spin orbit term (2.64). Still, $\hat{H}_2$ commutes with $\hat{L}^2$, $\hat{S}^2$ and the square of the total angular momentum $\hat{J}^2$ and its z-component $\hat{J}_z$. To the total angular momentum operator $\hat{J}$ belongs another quantum number j. Therefore, a change in set of quantum numbers is convenient when working with the spin-orbit coupling. On the Hamiltonian term (2.64) we perform a small trick to find a substitution for $\hat{\mathbf{L}}\cdot\hat{\mathbf{S}}$:

$$\hat{J}^2 = (\hat{\mathbf{L}} + \hat{\mathbf{S}})\cdot(\hat{\mathbf{L}} + \hat{\mathbf{S}}) = \hat{L}^2 + \hat{S}^2 + 2\hat{\mathbf{L}}\cdot\hat{\mathbf{S}} \tag{2.65}$$

$$\hat{\mathbf{L}}\cdot\hat{\mathbf{S}} = \frac{1}{2}(\hat{J}^2 - \hat{L}^2 - \hat{S}^2)\,, \tag{2.66}$$

and obtain a set of eigenvalues:

$$\frac{\hbar^2}{2}\Big[j(j+1) - l(l+1) - s(s+1)\Big] = \frac{\hbar^2}{2}\left[j(j+1) - l(l+1) - \frac{3}{4}\right]. \tag{2.67}$$

The spin of the electron is always $s = \frac{1}{2}$.
A correction to the energy levels is a consequence of the spin orbit interaction; splitting the levels depending on the value of the quantum number l. From perturbation theory this shift in energy levels for hydrogen is given by [21]:

$$\Delta E_2 = |E_n|\frac{\alpha^2}{n}\left(\frac{1}{j+\frac{1}{2}} - \frac{1}{l+\frac{1}{2}}\right) \qquad \text{where} \qquad j = l \pm \frac{1}{2}, \quad l \neq 0\,. \tag{2.68}$$

For $l = 0$ the spin orbit interaction vanishes.

Darwin Term

The last of the fine structure correction terms is the Darwin term. This correction only applies in the case $l = 0$, the s-state where the wave function is not zero at the origin, which means that there is a probability that the electron and the proton is at the same position. For all $l > 0$ states the wave function is zero at the origin and the Darwin term:

$$\hat{H}_3 = \frac{\pi\hbar^2}{2m^2c^2}\frac{e^2}{4\pi\epsilon_0}\delta(\mathbf{r}) \tag{2.69}$$

disappears. For $l = 0$ the correction to the relativistic energy takes the form:

$$\Delta E_3 = \frac{\pi\hbar^2}{2m^2c^2}\frac{e^2}{4\pi\epsilon_0}\langle\psi_{n00}|\delta(\mathbf{r})|\psi_{n00}\rangle \tag{2.70}$$

$$= \frac{\pi\hbar^2}{2m^2c^2}\frac{e^2}{4\pi\epsilon_0}|\psi_{n00}(0)|^2\,. \tag{2.71}$$

Where $|\psi_{n00}(0)|^2$ is the probability of finding the electron at the origin. The total relativistic Hamiltonian including the terms from equations (2.46), (2.53), (2.64) and (2.69) now reads:

$$\hat{H} = \hat{H}_0 + \hat{H}_1 + \hat{H}_2 + \hat{H}_3 \tag{2.72}$$

$$\hat{H} = \frac{\hat{p}^2}{2m} + V(r) - \frac{\hat{p}^4}{8m^3c^2} + \frac{e^2}{8\pi\epsilon_0}\frac{1}{m^2c^2r^3}\hat{\mathbf{L}}\cdot\hat{\mathbf{S}} + \frac{\pi\hbar^2}{2m^2c^2}\frac{e^2}{4\pi\epsilon_0}\delta(\mathbf{r})\,. \tag{2.73}$$

Taking all the energy corrections from the fine structure terms (equations (2.54) and (2.68)) and adding them together with the Bohr energy formula (2.44) gives the total energy for hydrogen:

$$E_{nj}^{TISE} = |E_n| + |E_n|\frac{\alpha^2}{n}\left(\frac{1}{j+\frac{1}{2}} - \frac{3}{4n}\right)\,, \tag{2.74}$$

because the $\frac{1}{l+1/2}$ terms cancel. Comparing this to the energy formula we get from solving the Dirac equation for a hydrogen atom [21]

$$E_{nj}^{Dirac} = \frac{mc^2}{\sqrt{1 + \frac{\alpha^2}{\left[n-j-\frac{1}{2}+\sqrt{(j+\frac{1}{2})^2-\alpha^2}\right]^2}}} - mc^2$$

$$= |E_n| + |E_n|\frac{\alpha^2}{n}\left(\frac{1}{j+\frac{1}{2}} - \frac{3}{4n}\right) + \mathcal{O}(\alpha^4) \tag{2.75}$$

where n and j are the principal quantum number and total angular momentum quantum number, respectively. α is the fine structure constant. We see that the energies are the same to order α^2

$$E_{nj}^{Dirac} = E_{nj}^{TISE} + \mathcal{O}(\alpha^4)\,. \tag{2.76}$$

Chapter 3

Hydrogen in an Electromagnetic Field

In this chapter we shall study the interaction between the hydrogen atom and an electromagnetic field. To take on such a task we will first present an overview of electrodynamics and the semi-classical approximation. A short introduction to the dipole approximation will be given before we study two different gauges for quantum mechanics: the so-called *velocity gauge* and *length gauge*. Our goal is to obtain relativistic Hamiltonians for hydrogen in an external field. The first section deals with the fundamentals of classical electrodynamics. The reader is referred to [22] for a good overview of the subject.

3.1 Maxwell's equations

It is impossible to talk about classical electrodynamics without introducing Maxwell's equations. James Clerk Maxwell was a Scottish physicist born in 1831. He was a multifaceted physicist, his publications spanning many fields from statistical physics to colour theory and optics. His first paper was published when he was only 14 years old [23]. When he published his famous equations he had 20 of them, in modern form they are reduced to 4 [24, 25]. Together with the force law,

$$\mathbf{F} = q(\mathbf{E} + \mathbf{v} \times \mathbf{B}) \tag{3.1}$$

the Maxwell's equations,

$$\begin{aligned} &i)\ \nabla\cdot\ \mathbf{E} = \frac{\rho}{\epsilon_0} && ii)\ \nabla\cdot\ \mathbf{B} = 0 \\ &iii)\ \nabla\times\ \mathbf{E} + \frac{\partial \mathbf{B}}{\partial t} = 0 && iv)\ \nabla\times\ \mathbf{B} - \mu_0\epsilon_0\frac{\partial \mathbf{E}}{\partial t} = \mu_0\mathbf{J} \end{aligned} \tag{3.2}$$

summarize our theoretical knowledge of electrodynamics. Here, they are stated for waves in vacuum. The Maxwell's equations describe how fields arise and depend on each other and the force law describes how charges move in electric and magnetic fields. Here, ρ is charge density, $\mathbf{E}$ and $\mathbf{B}$ are the electric and magnetic fields, respectively and $\mathbf{J}$ is the current area density. The constants μ_0 and ϵ_0 are the permeability and permittivity of vacuum, respectively. The Maxwell's equations describe how electric fields are produced either by the presence of charges or by changing magnetic fields. These properties are given by equation *i)* and *iii)*. Magnetic fields are produced by currents or changing electric fields, described by equation *ii)* and *iv)*. Writing the Maxwell's equations in this form

we keep the fields to the left and the sources of the fields to the right.

It is possible to reduce the four Maxwell's equations into two by using two substitutions: ϕ, the electric or scalar potential, and $\mathbf{A}$, the vector potential. We call these equations the potential representation

$$\mathbf{B}(\mathbf{r},t) = \nabla \times \mathbf{A}(\mathbf{r},t) \tag{3.3}$$

$$\mathbf{E}(\mathbf{r},t) = -\nabla\phi - \frac{\partial \mathbf{A}(\mathbf{r},t)}{\partial t}\,. \tag{3.4}$$

The equations (3.3) and (3.4) satisfy the Maxwell's equations (3.2) *ii*) and *iii*). Inserting equation (3.4) into *i*) and both (3.4) and (3.3) into *iv*) we get:

$$\nabla^2\phi + \frac{\partial}{\partial t}(\nabla \cdot \mathbf{A}(\mathbf{r},t)) = -\frac{\rho}{\epsilon_0} \tag{3.5}$$

$$\left(\nabla^2\mathbf{A}(\mathbf{r},t) - \mu_0\epsilon_0\frac{\partial^2\mathbf{A}(\mathbf{r},t)}{\partial t^2}\right) - \nabla\left(\nabla\cdot\mathbf{A}(\mathbf{r},t) + \mu_0\epsilon_0\frac{\partial\phi}{\partial t}\right) = -\mu_0\mathbf{J}\,. \tag{3.6}$$

Now we have reduced the information in Maxwell's 4 equations down to just 2 equations.

3.2 The semi-classical approximation

Studying the interaction of electromagnetic fields with atomic systems purely quantum mechanically requires the knowledge of quantum electrodynamics. To simplify the problem we use the semi-classical approximation, which means that we treat the electromagnetic fields classically by Maxwell's equations while the atomic system in question is treated quantum mechanically. We can apply this approximation because we are dealing with high photon densities from a laser. Even if the field is weak the photon density can be very high. For processes involving only a single photon, such as e.g. spontaneous emission, we must apply quantum field theory [26].

When applying an electromagnetic field to a charged particle there must be an alteration of the Hamiltonian. To find the Hamiltonian we need to know the Lagrangian of the system. A particle of mass m, charge q and velocity $\mathbf{v}$ in an electromagnetic field expressed by $\mathbf{A}$, is subjected to the Lorentz force given by equation (3.1). Inserting the equations (3.3) and (3.4) into (3.1) gives:

$$\mathbf{F} = q\Big(-\nabla\phi - \frac{\partial\mathbf{A}}{\partial t} + \mathbf{v}\times(\nabla\times\mathbf{A})\Big)\,. \tag{3.7}$$

We require that the Lagrangian produces the equations of motion satisfying (3.7). This is accomplished by the Lagrangian:

$$L = T - V = \frac{1}{2}mv^2 - q\phi + q\mathbf{v}\cdot\mathbf{A}\,. \tag{3.8}$$

If we work with Cartesian coordinates; our generalized coordinates are $q_1 = x$, $q_2 = y$ and $q_3 = z$. The generalized momentum is defined as:

$$p_i = \frac{\partial L}{\partial \dot{q}_i}\,, \tag{3.9}$$

where $p_1 = p_x$, $p_2 = p_y$ and $p_3 = p_z$ make up the components of $\mathbf{p}$. By inserting the Lagrangian and performing the derivation, the generalized momentum and an expression for the velocity can be found

$$\mathbf{p} = m\mathbf{v} + q\mathbf{A} \qquad \rightarrow \qquad \mathbf{v} = \frac{\mathbf{p} - q\mathbf{A}}{m}\,. \tag{3.10}$$

Since the Hamiltonian is defined as:

$$H = \sum_{i=1}^{3} p_i \dot{q}_i - L\,, \tag{3.11}$$

inserting the Lagrangian (3.8) and substituting in the expression for $\mathbf{v}$ from (3.10) the Hamiltonian in terms of $\mathbf{p}$, $\mathbf{A}$ and ϕ becomes [21]:

$$H = \frac{1}{2m}(\mathbf{p} - q\mathbf{A})^2 + q\phi\,. \tag{3.12}$$

The term $q\phi$ is set to zero when there are no charges affecting the field. This coupling between the momentum and the vector potential is called *minimal coupling*. The same result can be obtained by direct substitution of

$$\mathbf{p} \rightarrow \mathbf{p} - q\mathbf{A} \tag{3.13}$$

in a field free Hamiltonian. The charge affected by the field is the charge of the electron: $q = -e$. From classical mechanics the angular momentum is: $\mathbf{L} = \mathbf{r} \times \mathbf{p}$ and the momentum being coupled to the electromagnetic field gives $\mathbf{L} = \mathbf{r} \times (\mathbf{p} - q\mathbf{A})$. If we perform these substitutions on the relativistic Hamiltonian (2.73) for hydrogen from the previous chapter we obtain:

$$\begin{aligned}\hat{H}_{rel} =& \frac{(\hat{\mathbf{p}} + e\mathbf{A})^2}{2m} + V(r) - \frac{(\hat{\mathbf{p}} + e\mathbf{A})^4}{8m^3c^2} \\ &+ \frac{e^2}{8\pi\epsilon_0}\frac{1}{m^2c^2r^3}\big(\mathbf{r} \times (\hat{\mathbf{p}} + e\mathbf{A})\big) \cdot \hat{\mathbf{S}} + \frac{\pi\hbar^2}{2m^2c^2}\frac{e^2}{4\pi\epsilon_0}\delta(\mathbf{r})\,.\end{aligned} \tag{3.14}$$

In the non-relativistic limit, the correction terms vanish and the Hamiltonian can be written:

$$\hat{H}_{nonrel} = \frac{(\hat{\mathbf{p}} + e\mathbf{A})^2}{2m} + V(r) \tag{3.15}$$

3.2.1 The dipole approximation

A common approximation used when modeling atoms in an electromagnetic field is the dipole approximation. For this approximation we assume that the wavelength of the laser field is much longer than the extent of the whole atom so that the field can be accounted as uniform over our system i.e. $\lambda \gg 1$Å. Thus, the field becomes space-independent:

$$\mathbf{A}(\mathbf{r}, t) \rightarrow \mathbf{A}(t)\,. \tag{3.16}$$

This also requires that the laser intensity is not too high. Neglecting space dependence in $\mathbf{A}$ also means neglecting the magnetic field, a consequence of equation (3.3).
Expanding the parenthesis in the Hamiltonian (3.15) yields:

$$\hat{H}_{nonrel} = \frac{\hat{p}^2}{2m} + \frac{e(\mathbf{A}\cdot\hat{\mathbf{p}})}{m} + \frac{e^2\mathbf{A}^2}{2m} + V(r)\,, \tag{3.17}$$

where we have imposed the so-called Coulomb gauge where $\hat{\mathbf{p}}\cdot\mathbf{A} = \mathbf{A}\cdot\hat{\mathbf{p}}$. Within the dipole approximation the so-called diamagnetic term $\frac{e^2\mathbf{A}^2}{2m}$ disappears if we perform the following gauge transformation on our wave function:

$$\Psi(\mathbf{r},t) \to \Psi(\mathbf{r},t)e^{-i\frac{e^2}{2m}\int_0^t \mathbf{A}^2(t')dt'}\,. \tag{3.18}$$

After this transformation has been performed; the non-relativistic Hamiltonian,

$$\hat{H}_{nonrel} = \frac{\hat{p}^2}{2m} + \frac{e(\mathbf{A}\cdot\hat{\mathbf{p}})}{m} + V(r)\,, \tag{3.19}$$

is now said to be in the *velocity gauge*. The name *velocity gauge* comes from the fact that the field is coupled to the velocity operator $\frac{\hat{\mathbf{p}}}{m}$.

3.3 Gauge transformations

Quantum mechanics is gauge invariant, which means that any gauge must produce the same results for the observables. Certain changes of the electric potential and the vector potential can be done as long as they do not cause the physical fields to change. Transformations of the potentials that are non-observable are called gauge transformations. For the electric potential this means that we can add the time derivative of any real differentiable scalar function $\chi(\mathbf{r},t)$,

$$\phi(\mathbf{r},t) \to \phi(\mathbf{r},t) - \frac{\partial\chi(\mathbf{r},t)}{\partial t}\,. \tag{3.20}$$

Substituting this into (3.4) we see that the gradient of a time derivative is zero and the electric field remains unchanged.

Similarly for the vector potential, we can perform the gauge transformation:

$$\mathbf{A}(\mathbf{r},t) \to \mathbf{A}(\mathbf{r},t) + \nabla\chi \tag{3.21}$$

and we see from equation (3.3) that the curl of a gradient is zero and the magnetic field is unchanged.

3.3.1 Velocity gauge and length gauge

The relativistic Hamiltonian (3.14) can be transformed using the gauge transformation [21]:

$$\begin{aligned}
\mathbf{A}(\mathbf{r},t) =& \mathbf{A}'(\mathbf{r},t) + \nabla\chi(\mathbf{r},t) \\
\phi(\mathbf{r},t) =& \phi'(\mathbf{r},t) - \frac{\partial}{\partial t}\chi(\mathbf{r},t) \\
\Psi(\mathbf{r},t) =& \Psi'(\mathbf{r},t)e^{iq\chi(\mathbf{r},t)/\hbar}\,.
\end{aligned} \tag{3.22}$$

Since we are working in the dipole approximation the scalar potential and the vector potential in the velocity gauge are:

$$\begin{aligned} \phi &= 0 \\ \mathbf{A} &= \mathbf{A}(t)\,. \end{aligned} \tag{3.23}$$

By performing a gauge transformation with the following properties:

$$\begin{aligned} \chi(\mathbf{r},t) &= \mathbf{A}(t)\cdot\mathbf{r} \\ \mathbf{E}(t) &= -\,\frac{d\mathbf{A}(t)}{dt}\,, \end{aligned} \tag{3.24}$$

we can see from using the equations (3.22) that the relations become the following now that $\mathbf{A}(\mathbf{r},t) \to \mathbf{A}(t)$:

$$\begin{aligned} \mathbf{A}'(t) =& \mathbf{A}(t) - \nabla\left(\mathbf{A}(t)\cdot\mathbf{r}\right) = 0 \\ \phi'(\mathbf{r},t) =& \phi(\mathbf{r},t) + \frac{\partial}{\partial t}\mathbf{A}(t)\cdot\mathbf{r} = -\mathbf{E}(t)\cdot\mathbf{r} \\ \Psi'(\mathbf{r},t) =& \Psi(\mathbf{r},t)e^{-iq\mathbf{A}(t)\cdot\mathbf{r}/\hbar}\,. \end{aligned} \tag{3.25}$$

Looking back at the relativistic Hamiltonian (3.14) in velocity gauge we see that all the terms involving $\mathbf{A}(t)$ become zero but the term $q\phi$ is no longer zero because $\phi'(\mathbf{r},t) = -\mathbf{E}(t)\cdot\mathbf{r}$. This transformation gives us the following relativistic Hamiltonian:

$$\hat{H}'_{rel} = \frac{\hat{p}^2}{2m} + V(r) - \frac{\hat{p}^4}{8m^3c^2} + \frac{e^2}{8\pi\epsilon_0}\frac{1}{m^2c^2r^3}\hat{\mathbf{L}}\cdot\hat{\mathbf{S}} + \frac{\pi\hbar^2}{2m^2c^2}\frac{e^2}{4\pi\epsilon_0}\delta(\mathbf{r}) + e\mathbf{E}(t)\cdot\mathbf{r}\,, \tag{3.26}$$

for hydrogen. The field is no longer present in the spin-orbit coupling like in the velocity gauge. This gauge is the so-called *length gauge* because the interaction term couples the electric field and the position. In the non-relativistic limit the correction terms vanish and we get the Hamiltonian:

$$\hat{H}'_{nonrel} = \frac{\hat{p}^2}{2m} + V(r) + e\mathbf{E}(t)\cdot\mathbf{r}\,, \tag{3.27}$$

for hydrogen in length gauge. The motivation for obtaining the Hamiltonian in the two different gauges (3.14) and (3.26), respectively, will be clarified in a later chapter.

Chapter 4

Numerical Approach to Solving the Schrödinger Equation

Quantum mechanical systems are notorious for their complex and lengthy calculations for even quite simple systems. The possibility of solving the Schrödinger equation analytically quickly fades and we must enter into the realm of numerical methods. In this chapter the numerical methods used for the calculations in this thesis will be presented. This includes a section on B-splines as basis functions, the Gauss-Legendre integration method and the calculation of the relativistic corrections' matrix elements.

4.1 Solving the non-relativistic Schrödinger equation numerically

The time independent Schrödinger equation,

$$\hat{H}\psi = E\psi\,, \tag{4.1}$$

can be solved as an eigenvalue problem. Analytically, the set of wave functions and eigenstates is infinite. Numerically, we truncate our set at a finite number of energy states, $k \in \{1, 2, ..., N_{max}\}$, per value of the quantum numbers $l \in \{0, 1, ..., l_{max}\}$ and $m \in \{-l, -l+1, ..., 0, ..., l-1, l\}$. Separation of variables gives the following expression for the wave function:

$$\psi_{klm}(\mathbf{r}) = \frac{\mathcal{U}_{kl}(r)}{r} Y_{lm}(\theta, \phi)\,, \tag{4.2}$$

where $Y_{lm}(\theta, \phi)$ is the spherical harmonic function and the $R(r) = \frac{\mathcal{U}_{kl}(r)}{r}$ is the radial function, which is a solution of equation (2.43) from the second chapter:

$$\left[-\frac{\hbar^2}{2m}\frac{d^2}{dr^2} + V(r) + \frac{\hbar^2}{2m}\frac{l(l+1)}{r^2} \right] \mathcal{U}_{kl}(r) = E\,\mathcal{U}_{kl}(r)\,. \tag{4.3}$$

As discussed in chapter 2 the problem can be expressed as a matrix equation,

$$\begin{bmatrix} H_{11} & H_{12} & \dots & H_{1q} \\ H_{21} & H_{22} & \dots & H_{2q} \\ \vdots & \vdots & \ddots & \vdots \\ H_{p1} & H_{p2} & \dots & H_{p,q} \end{bmatrix} \begin{bmatrix} \mathcal{U}_1 \\ \mathcal{U}_2 \\ \vdots \\ \mathcal{U}_q \end{bmatrix} = E \begin{bmatrix} \mathcal{U}_1 \\ \mathcal{U}_2 \\ \vdots \\ \mathcal{U}_q \end{bmatrix} \tag{4.4}$$

where the matrix elements can be written as:

$$H_{pq} = \int_{-\infty}^{\infty} \mathcal{U}_p^*(r)\ \hat{H}\ \mathcal{U}_q(r,)\ dr\,. \tag{4.5}$$

Diagonalization of the Hamiltonian matrix gives the energy eigenvalues and the corresponding eigenstates of the system. To shorten the notation the indices $p = \{kl\}$ and $q = \{k'l'\}$ are adopted. p and q contain the energy state and quantum number l of the electron and describes the placement in the matrix. It will only be necessary to calculate the radial integrals numerically while the angular integrals can be calculated analytically. As a consequence of this we do not need to resolve the spherical harmonics numerically, but the radial functions must be computed in order to solve the radial integrals. The radial functions will be expressed as a linear combination of basis functions.

4.2 B-splines

For our calculations of the radial function we shall use a basis of B-splines [27]. B-splines are polynomial functions non-zero and non-negative at a certain interval. They are distributed over the box in which we define our wave functions. The box is defined by the interval $I = [0, r_{max}]$ where the radial coordinate r vary between 0 and the extent of the box, r_{max}. More information on B-splines and their application in atomic physics can be found in [28].

The box interval, $I = [0, r_{max}]$, is divided into subintervals $\{0, r_1, ..., r_n, ..., r_{max=N_r}\}$ by a sequence of breakpoints. To each breakpoint we assign a number of knots. The endpoints of the box are given a multiplicity of k knots. For the inner breakpoints we restrict ourselves to one knot per breakpoint. In total there is a set of m knots: $\{t_i\}_{i=1,2...m}$.
Each B-spline is defined over an interval $[t_i, t_{i+k}]$ of $k+1$ knots. An interval between two consecutive knots therefore contain k number of B-splines. The total number of B-splines N_B is then $N_B = m - k$. They are normalized such that the sum of the B-spline values at a point r is 1 i.e. $\sum_i B_i(r) = 1$.

The first order spline is defined to be 1 or 0 depending on whether our point is located in the B-splines' defined interval.

$$B_i^1(r) = 1 \qquad \text{if} \qquad t_i \leq r < t_{i+1} \qquad \text{and} \qquad B_i^1 = 0 \qquad \text{otherwise.} \tag{4.6}$$

Note that this corresponds to a zeroth order polynomial. The higher order splines are then generated by the following recursion relation using the splines of previous order:

$$B_i^k(r) = \frac{r - t_i}{t_{i+k-1} - t_i} B_i^{k-1}(r) + \frac{t_{i+k} - r}{t_{i+k} - t_{i+1}} B_{i+1}^{k-1}(r)\,. \tag{4.7}$$

The splines derivatives can also be calculated using a similar recursion relation:

$$\frac{d}{dr} B_i^k(r) = \frac{k-1}{t_{i+k-1} - t_i} B_i^{k-1}(r) - \frac{k-1}{t_{i+k} - t_{i+k}} B_{i+1}^{k-1}(r)\,. \tag{4.8}$$

Repeating the process using the new obtained derivatives gives higher order derivatives. For our calculations we only require first and second order derivatives.

Figure 4.1 shows a set of $m - k = 17 - 4 = 13$ B-splines on the interval $[0, r_{max}] = [0, 10]$ with spacing 1 between the breakpoints. The end breakpoints have a multiplicity of 4 knots and the intermediate points have 1 knot each.

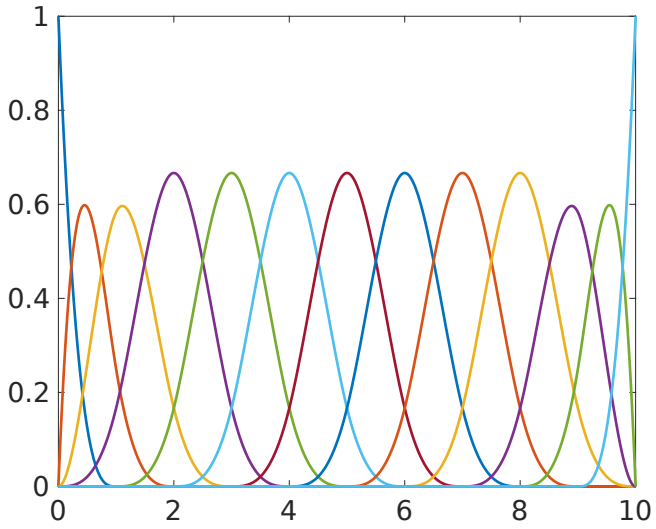

Figure 4.1: [B-splines 0,r_{max}]=[0,10] with 17 knots and order 4.

In all calculations we shall remove the first and last B-spline in order to satisfy the boundary conditions. The proper number of B-splines is then $N_B = m - k - 2$.

4.2.1 Using B-splines to solve the radial equation

Our mission is to solve the Schrödinger equation and the first step is to obtain the energy levels for hydrogen. We start by examining the radial equation from (4.3) and insert the Coulomb potential $V(r) = -\frac{e^2}{4\pi\epsilon_0 r}$:

$$\left[-\frac{\hbar^2}{2m}\frac{d^2}{dr^2} + \frac{\hbar^2 l(l+1)}{2mr^2} - \frac{e^2}{4\pi\epsilon_0 r} \right] \mathcal{U}_{kl}(r) = E_k \, \mathcal{U}_{kl}(r) \, . \tag{4.9}$$

The boundary conditions are $\mathcal{U}_{kl}(r = 0) = 0$ and
$\mathcal{U}_{kl}(r = r_{max}) = 0$. The solution can now be expanded on the B-spline basis set:

$$\mathcal{U}_{kl}(r) = \sum_{i=1}^{N_B} c_i^{kl} B_i(r) \, . \tag{4.10}$$

Inserting this into equation (4.9) yields:

$$\left[-\frac{\hbar^2}{2m}\frac{d^2}{dr^2} + \frac{\hbar^2 l(l+1)}{2mr^2} - \frac{e^2}{4\pi\epsilon_0 r} \right] \sum_{i=1}^{N_B} c_i^{kl} B_i(r) = E_k \sum_{i=1}^{N_B} c_i^{kl} B_i(r) \, . \tag{4.11}$$

The basis depends on the following parameters: the box size, the order of the basis set k and the number of B-splines, N_B, on the interval I. These parameters must be chosen in accordance with the problem we want to solve.

If we are considering a specific angular momentum l the problem can be recognized as an eigenvalue problem:

$$\begin{bmatrix} H_{11} & H_{12} & \dots & H_{1N_B} \\ H_{21} & H_{22} & \dots & H_{2N_B} \\ \vdots & \vdots & \ddots & \vdots \\ H_{N_B1} & H_{N_B2} & \dots & H_{N_B,N_B} \end{bmatrix} \begin{bmatrix} c_1 \\ c_2 \\ \vdots \\ c_{N_B} \end{bmatrix} = E \begin{bmatrix} S_{11} & S_{12} & \dots & S_{1N_B} \\ S_{21} & S_{22} & \dots & S_{2N_B} \\ \vdots & \vdots & \ddots & \vdots \\ S_{N_B1} & S_{N_B2} & \dots & S_{N_B,N_B} \end{bmatrix} \begin{bmatrix} c_1 \\ c_2 \\ \vdots \\ c_{N_B} \end{bmatrix}, \tag{4.12}$$

which is equivalent to solving a system of N_B linear equations. The matrix S is the overlap matrix; which is needed because the B-splines do not form an orthonormal set of basis functions. The matrix elements for a certain l are calculated from the integrals

$$H^l_{ij} = \int_0^{r_{max}} B_i(r) \left[-\frac{\hbar^2}{2m}\frac{d^2}{dr^2} + \frac{\hbar^2 l(l+1)}{2m}\frac{1}{r^2} - \frac{e^2}{4\pi\epsilon_0}\frac{1}{r} \right] B_j(r) dr \,, \tag{4.13}$$

and the overlap matrix is calculated from the integrals

$$S_{ij} = \int_0^{r_{max}} B_i(r) B_j(r) dr \,. \tag{4.14}$$

The integrals are calculated using the Gauss-Legendre integration method, also called the Gauss-Legendre quadrature. The approach of the method is to approximate an integral by performing a finite sum given by the equation:

$$\int_{r_n}^{r_{n+1}} f(r)dx \;\approx\; \frac{r_{n+1}-r_n}{2} \sum_{a=1}^{k} w_a f\left(\frac{r_{n+1}-r_n}{2}\lambda_a + \frac{r_n + r_{n+1}}{2} \right), \tag{4.15}$$

where r_n and r_{n+1} are two consecutive breakpoints. For the Gauss-Legendre quadrature the idea is to pick a set of weights, w_a, and a set of nodes, r_a, to get the most optimal result. For the above integral: if $f(r)$ is any polynomial of degree d and we are using k (order) integration points which satisfies $d \leq 2k-1$, then the finite sum gives the exact value of the integral. A product of two B-splines will give polynomials of degree $d = 2k-2$ at most and the condition is satisfied. The optimal set of nodes and weights are obtained from the zeroes of the Legendre polynomial. We set up the $k \times k$ Jacobi matrix J for Legendre polynomials. The entries of the matrix J are described in [29] as:

$$\alpha_a = 0, \qquad \beta_a = \frac{1}{2}\left(1 - (2a)^{-2}\right)^{-\frac{1}{2}} \,. \tag{4.16}$$

where $\alpha_1, ..., \alpha_k$ are diagonal elements and $\beta_1, ...\beta_{k-1}$ are tridiagonal elements. The Jacobi matrix can be written $J = VDV^T$, where V is the matrix containing the eigenvectors, v_a, and D is a diagonal matrix of the eigenvalues, λ_a. From the following relations; the nodes are calculated from the eigenvalues of the Jacobi matrix and the weights are found using the eigenvectors:

$$r_a = \frac{r_{n+1}-r_n}{2}\lambda_a + \frac{r_n + r_{n+1}}{2} \tag{4.17}$$

$$w_a = 2(v_a)_1^2 \qquad a = 1, 2, ..., k \,, \tag{4.18}$$

where $(v_a)_1$ is the first element of each eigenvector. The B-splines are generated using the nodes, r_a, for each knot interval. Further, the integration over the entire box is

performed by summing the integrations over each knot point interval. The integrations are performed using the Gauss-Legendre integration with the weights. Equations (4.13) and (4.14) then become:

$$H_{ij}^{l} = \sum^{m-1} \int_{t_n}^{t_{n+1}} B_i(r) \left[-\frac{\hbar^2}{2m}\frac{d^2}{dr^2} + \frac{\hbar^2 l(l+1)}{2m}\frac{1}{r^2} - \frac{e^2}{4\pi\epsilon_0}\frac{1}{r} \right] B_j(r) dr \,, \tag{4.19}$$

$$S_{ij} = \sum^{m-1} \int_{t_n}^{t_{n+1}} B_i(r) B_j(r) dr \,. \tag{4.20}$$

The integrals containing the kinetic energy term can be calculated exactly using this method, but the Coulomb potential term and the centrifugal term are rational functions for which the above statement does not hold. Although these integrals will not be computed exactly, they still prove to be very accurate.

4.3 Calculation of the relativistic corrections

The Hamiltonian matrix in (4.12) can now be diagonalized to obtain the energy eigenvalues, E_k^0, for the non-relativistic hydrogen atom for both bound and pseudo-continuum states. The eigenvectors or reduced radial functions $\mathcal{U}_{kl}^0(r)$ are also obtained. The total non-relativistic wave function is described as $\psi_{klm}^0(\mathbf{r}) = \frac{\mathcal{U}_{kl}^0(r)}{r} Y_{lm}^0(\theta,\phi)$. The diagonalization of the Hamiltonian is performed using the *eig*-function in MATLAB. The number of eigenvalues equal the number of B-splines, N_B, used in the calculation. Truncation of the number of eigenvalues is determined by how high energies we want to study.

Starting off with N_B eigenvalues after the diagonalization; not all these are considered reliable due to the B-splines not being able to approximate fast oscillating functions very well. As a rule of thumb we then use: $N_l \approx \frac{N_B}{2}$. The orbital angular momentum quantum number is truncated at l_{max}, thus obtaining the total Hamiltonian matrix $\hat{H}$ in equation (4.4) of dimension $(l_{max}+1)\cdot N_l \times (l_{max}+1)\cdot N_l$.

We now return to the relativistic Hamiltonian (2.73) stated in chapter 2:

$$\hat{H} = \frac{\hat{p}^2}{2m} + V(r) - \frac{\hat{p}^4}{8m^3c^2} + \frac{e^2}{8\pi\epsilon_0}\frac{1}{m^2c^2r^3}\hat{\mathbf{L}}\cdot\hat{\mathbf{S}} + \frac{\pi\hbar^2}{2m^2c^2}\frac{Ze^2}{4\pi\epsilon_0}\delta(\mathbf{r}) \,. \tag{4.21}$$

The first two terms have now been implemented and the remaining terms are the three relativistic corrections. They all provide corrections to the energy levels of the hydrogen atom as seen in chapter 2 from equations (2.54), (2.68) and (2.71). We start with the implementation of the correction to the kinetic energy of the hydrogen atom:

$$\hat{H}_1 = -\frac{\hat{p}^4}{8m^3c^2} \,. \tag{4.22}$$

The optimal approach for the calculation of these integrals was to make the substitution:

$$\frac{\hat{p}^2}{2m} = \hat{H}_0 - V(r) \,. \tag{4.23}$$

Applying this yields:

$$H_{pq}^{p^4} = -\frac{1}{2mc^2}\left\langle \left(\hat{H}_0 - V(r)\right)\frac{\mathcal{U}_{kl}^0}{r}Y_{lm}^0 \,\middle|\, \left(\hat{H}_0 - V(r)\right)\frac{\mathcal{U}_{k'l'}^0}{r}Y_{l'm'}^0 \right\rangle \tag{4.24}$$

We already know that $\hat{H}_0$ acting on the wave function produces the energy eigenvalues E_n^0. Further calculations and separation of the wave function yields:

$$H_{pq}^{p^4} = -\frac{1}{2mc^2}\delta_{ll'}\ \delta_{mm'}\int_0^{r_{max}}\left[E_k^0 E_{k'}^0 + \frac{E_k^0}{r} + \frac{E_{k'}^0}{r} + \frac{1}{r^2}\right]\mathcal{U}_{kl}^0\ \mathcal{U}_{k'l'}^0\, dr\,. \tag{4.25}$$

The δ are the Kronecker delta; taking the value 1 when the value of the indices are equal and 0 when they are different. From the Kronecker delta we see that this term only couples states of the same orbital angular momentum and magnetic quantum number.

The Darwin term does not require us to perform any integral because it depends only on the value of the wave function at the origin,

$$H_{pq}^{D} = \frac{\pi\hbar^2}{2m^2c^2}\frac{e^2}{4\pi\epsilon_0}|\psi_{k00}(0)|^2\,, \tag{4.26}$$

which is found by extrapolating the wave function to origo using the MATLAB *spline*-function. Note that the Darwin term only provides a correction when $l = 0$.

When $l > 0$ the LS-coupling takes over. The eigenvalues to the LS-coupling are known from chapter 2 in equation (2.67)

$$\frac{\hbar^2}{2}\Big[j(j+1) - l(l+1) - s(s+1)\Big]\,. \tag{4.27}$$

The total integral for the calculation of the LS-coupling matrix elements become:

$$H_{pq}^{LS} = \frac{\hbar}{16\pi\epsilon_0 m^2c^2}\Big[j(j+1) - l(l+1) - s(s+1)\Big]\int_0^{r_{max}}\frac{1}{r^3}\,\mathcal{U}_{kl}\,\mathcal{U}_{k'l'}dr\,, \tag{4.28}$$

where j is the total angular momentum quantum number. The permitted values for j is given by the Clebsch-Gordan series [18]:

$$j = j_1 + j_2, j_1 + j_2 - 1, ..., |j_1 - j_2|\,, \tag{4.29}$$

where for a particle like the electron we have $j_1 = l$, the orbital angular momentum, and $j_2 = s$, the spin. The spin being known gives the following possible values for j:

$$j = \frac{1}{2} \qquad \text{for } l = 0\,, \tag{4.30}$$

$$j_+ = l + \frac{1}{2}, \qquad j_- = \left|l - \frac{1}{2}\right| \qquad \text{for } l > 0\,. \tag{4.31}$$

Two sets of energy eigenvalues, one for each j, is obtained when $l > 0$. To include the total angular momentum j we must make a change of scheme to where it can be determined. So far we have essentially been working in the so-called uncoupled picture. The two different pictures (coupled and uncoupled) have different sets of quantum numbers that can be specified. In the uncoupled picture we are assuming that the quantum numbers

l, s, m_l, m_s can be determined, but the total angular momentum j cannot be specified in this picture. We write the uncoupled states as

$$|l, m_l\rangle|s, m_s\rangle \,. \tag{4.32}$$

Turning to the coupled picture we can determine j and the sum of the magnetic quantum number and the spin projection quantum number: $m_j = m_l + m_s$, but not the individual components m_l and m_s. The coupled states can be written:

$$|ls, jm_j\rangle \,. \tag{4.33}$$

The relation between the coupled and uncoupled states is given by:

$$|jm_j, ls\rangle = \sum_{m_l, m_s} C(m_l, m_s)|l, m_l\rangle|s, m_s\rangle \,, \tag{4.34}$$

where the coefficients $C(m_l, m_s)$ are the Clebsch Gordan coefficients [18] given by the inner product:

$$C(m_l, m_s) = \langle lm_l, sm_s|jm_j, ls\rangle \,. \tag{4.35}$$

We perform a second diagonalization of the new Hamiltonian containing the previously calculated energy values along the diagonal and the new obtained matrix elements from the integrals above. New energy eigenvalues, E_k, with relativistic correction and corrected wave functions $\psi_{klm} = \frac{\mathcal{U}_{kl}}{r} Y_{lm}$ are obtained.

Table (4.1) show the energy levels of hydrogen for the s-states, $l = 0$, for the non-relativistic and the relativistic calculation. The calculation has been performed using a box of size 160 a.u. and 900 6th order basis functions.

Comparing the calculated energies with the energies obtained from the formulas in chapter 2, (2.44), (2.74) and (2.75), we can see that our obtained energies are in good agreement with the results from the formulas at least down to 8 decimals. The non-relativistic energies have shown to be precise to 13 decimals. In the table we use 9 decimals, this is the order of agreement between the formulas (2.74) and (2.75).

	Non-relativistic, Bohr energy (2.44)	Non-relativistic calculated	Relativistic from formulas (2.74) (2.75)	Relativistic calculated
1s	-0.5	-0.500000000	-0.500006656	-0.500006664
2s	-0.125	-0.125000000	-0.125002080	-0.125002081
3s	-0.055555556	-0.055555556	-0.055556295	-0.055556296
4s	-0.03125	-0.031249999	-0.031250338	-0.031250338
5s	-0.02	-0.020000000	-0.020000181	-0.020000181

Table 4.1: Non-relativistic and relativistic energy levels in hydrogen.

Chapter 5

Photoionization of Hydrogen - a Time Independent Study

The results section will be split into two separate parts. This part presents a time independent study of the photoionization cross section of the electron in a weak field. Cross section describes the area in which all the projectile particles that enter through said area will be scattered off the target in some direction. In other words, the area of the target particle as experienced by the projectile particle. A photon of energy E might hit our electron and cause it to either be excited to a higher bound state or ionize the atom. We shall study the interaction between $1s$ and kp states; the electron's transition from the ground state to continuum states that have orbital quantum number $l = 1$. This is a single photon interaction and only transitions with $\Delta l = \pm 1$ are allowed.

Inspecting the two Hamiltonians with relativistic corrections in the two different gauges that we found in chapter 3 i.e., the velocity gauge relativistic Hamiltonian (3.14) and the length gauge relativistic Hamiltonian (3.26), we note that the length gauge Hamiltonian has some advantages for this type of calculations, in that it has only one interaction term,

$$\hat{H}_{int} = e\mathbf{E}(t) \cdot \mathbf{r}\,. \tag{5.1}$$

The relativistic length gauge Hamiltonian (3.26):

$$\begin{aligned}\hat{H} =& \frac{\hat{p}^2}{2m} + V(r) - \frac{\hat{p}^4}{8m^3c^2} + \frac{e^2}{8\pi\epsilon_0}\frac{1}{m^2c^2r^3}\hat{\mathbf{L}}\cdot\hat{\mathbf{S}} \\ &+ \frac{\pi\hbar^2}{2m^2c^2}\frac{e^2}{4\pi\epsilon_0}\delta(\mathbf{r}) + e\mathbf{E}(t)\cdot\mathbf{r}\,,\end{aligned} \tag{5.2}$$

will therefore be used in the calculation of the photoionization cross section.

5.1 Finding an expression for the cross section in length gauge

To find an expression for the cross section we turn to time dependent perturbation theory. In the study of the single photon absorption process we will treat the interaction term (5.1) as a small perturbation. The transitions we are studying have well defined initial and final states α and β. Starting with the time dependent Schrödinger equation:

$$i\hbar\frac{\partial}{\partial t}\Psi(\mathbf{r},t) = \hat{H}\Psi(\mathbf{r},t) = \left(\hat{H}_0 + \hat{H}_{int}\right)\Psi(\mathbf{r},t)\,, \tag{5.3}$$

where $\hat{H}_0$ is the Hamiltonian (2.73) and the eigenvalues of the Hamiltonian $\hat{H}_0$ are known,

$$\hat{H}_0\psi_k = E_k\psi_k\,. \tag{5.4}$$

The general solution of the time dependent Schrödinger equation can be written:

$$\Psi(\mathbf{r},t) = \sum_k c_k(t)\psi_k(\mathbf{r})e^{-iE_kt/\hbar}\,. \tag{5.5}$$

The general solution is inserted in the TDSE and the perturbation is switched on at $t = 0$. The transition amplitude for the final state, β, in first order time dependent perturbation theory is given by:

$$c_\beta(t) = \frac{1}{\hbar}\int_0^t \left\langle \psi_\beta\middle|\hat{H}_{int}\middle|\psi_\alpha\right\rangle e^{i\omega_{\beta\alpha}t'}dt'\,, \tag{5.6}$$

where the energy difference of the initial and final state of the electron equals the energy of the absorbed photon, $E_\beta - E_\alpha = \omega_{\beta\alpha}\hbar$. Since we are applying the dipole approximation, the electric field in our perturbation is described as a plane wave,

$$\mathbf{E}(t) = E_0\sin(\omega t)\,, \tag{5.7}$$

i.e. our perturbation is harmonic and the electric field can be written as:

$$E_0\sin(\omega t) = \frac{E_0}{2i}\left(e^{i\omega t} - e^{-i\omega t}\right)\,. \tag{5.8}$$

The process of solving harmonic perturbations is described in [20].
When (5.8) is inserted in (5.6) we get:

$$\begin{aligned} c_\beta(t) =& \frac{1}{i\hbar}\left\langle \psi_\beta\middle|\frac{eE_0}{2i}\cdot\mathbf{r}\middle|\psi_\alpha\right\rangle\int_0^t e^{i(\omega_{\beta\alpha}+\omega)t'}dt' \\ =& -\frac{1}{i\hbar}\left\langle \psi_\beta\middle|\frac{eE_0}{2i}\cdot\mathbf{r}\middle|\psi_\alpha\right\rangle\int_0^t e^{i(\omega_{\beta\alpha}-\omega)t'}dt'\,, \end{aligned} \tag{5.9}$$

and the integrals in the transition amplitude can be solved so that we obtain:

$$\begin{aligned} c_\beta(t) =& \left\langle \psi_\beta\middle|\frac{eE_0}{2i}\cdot\mathbf{r}\middle|\psi_\alpha\right\rangle\frac{1-e^{i(\omega_{\beta\alpha}+\omega)t}}{\hbar\omega_{\beta\alpha}+\hbar\omega} \\ &-\left\langle \psi_\beta\middle|\frac{eE_0}{2i}\cdot\mathbf{r}\middle|\psi_\alpha\right\rangle\frac{1-e^{i(\omega_{\beta\alpha}-\omega)t}}{\hbar\omega_{\beta\alpha}-\hbar\omega} \end{aligned} \tag{5.10}$$

where the first part can be neglected when we are dealing with absorption where $\hbar\omega_{\beta\alpha} \simeq \hbar\omega$. If we take the square of the absolute value of the transition amplitude we get the transition probability:

$$P(t) = \left|c_\beta(t)\right|^2 = \left|\left\langle \psi_\beta\middle|\frac{eE_0}{2i}\cdot\mathbf{r}\middle|\psi_\alpha\right\rangle\right|^2\frac{\left|1-e^{i(\omega_{\beta\alpha}-\omega)t}\right|^2}{\left(\hbar\omega_{\beta\alpha}-\hbar\omega\right)^2}\,. \tag{5.11}$$

Using trigonometric identities gives:

$$P(t) = 4\left|\left\langle\psi_\beta\right|\frac{eE_0}{2i}\cdot\mathbf{r}\left|\psi_\alpha\right\rangle\right|^2\frac{\sin^2\left[\frac{(\hbar\omega_{\beta\alpha}-\hbar\omega)t}{2\hbar}\right]}{\left(\hbar\omega_{\beta\alpha}-\hbar\omega\right)^2}\,. \tag{5.12}$$

We make the substitution $x = \frac{\hbar\omega_{\beta\alpha}-\hbar\omega}{2\hbar}$ and multiply by $\frac{\pi}{\pi}$. The transition rate, $W(t) = \frac{P(t)}{t}$ can be written:

$$W(t) = 4\pi\left|\left\langle\psi_\beta\right|\frac{eE_0}{2i}\cdot\mathbf{r}\left|\psi_\alpha\right\rangle\right|^2\frac{\sin^2(xt)}{4\pi\hbar^2x^2t}\,. \tag{5.13}$$

From appendix B in [20] when time approaches infinity the expression:

$$\lim_{t\to\infty}\frac{1}{\pi t}\frac{\sin^2(xt)}{x^2} = \delta(x)\,, \tag{5.14}$$

can be approximated to the delta function. We therefore set the time to approach infinity for the transition rate:

$$W = \lim_{t\to\infty}\frac{P(t)}{t} = \frac{\pi}{\hbar^2}\left|\left\langle\psi_\beta\right|\frac{eE_0}{2i}\cdot\mathbf{r}\left|\psi_\alpha\right\rangle\right|^2\delta\left(\frac{\hbar\omega_{\beta\alpha}-\hbar\omega}{2\hbar}\right)\,. \tag{5.15}$$

Using appendix B in [20] again to find that $\delta\left(\frac{\hbar\omega_{\beta\alpha}-\hbar\omega}{2\hbar}\right) = 2\hbar\delta\left(\hbar\omega_{\beta\alpha}-\hbar\omega\right)$ we get the following expression:

$$W = \frac{2\pi}{\hbar}\left|\left\langle\psi_\beta\right|\frac{eE_0}{2i}\cdot\mathbf{r}\left|\psi_\alpha\right\rangle\right|^2\delta\left(\hbar\omega_{\beta\alpha}-\hbar\omega\right)\,. \tag{5.16}$$

This is the probability per unit time of a transition from the state α to the state β. We shall study transitions from the well defined ground state, 1s, to the continuum states by absorption of a photon of frequency ω. However, the number of continuum states on any energy interval in the continuum is infinite, but in order to be able to apply the transition rate formula we will define a number of states in our so-called pseudo-continuum. We define a number $\rho(E)dE$ of states on an interval $[E, E+dE]$, where the $\rho(E)$ is the density of states. To obtain the total transition rate we must integrate over all possible end states β:

$$W_{\beta\alpha} = \int_{-\infty}^{\infty}W(E_\beta)\rho(E_\beta)dE_\beta \tag{5.17}$$

$$= \frac{2\pi}{\hbar}\int_{-\infty}^{\infty}\left|\left\langle\psi_\beta\right|\frac{eE_0}{2i}\cdot\mathbf{r}\left|\psi_\alpha\right\rangle\right|^2\rho(E_\beta)\delta\left(\hbar\omega_{\beta\alpha}-\hbar\omega\right)dE_\beta\,. \tag{5.18}$$

This yields the famous Fermi's Golden Rule which describes the transition rate from a bound state to the continuum:

$$W_{\beta\alpha} = \frac{2\pi}{\hbar}\left|\left\langle\psi_\beta\right|\frac{eE_0}{2i}\cdot\mathbf{r}\left|\psi_\alpha\right\rangle\right|^2\rho(E_\beta)\,, \tag{5.19}$$

where $E_\beta = E_\alpha + \hbar\omega_{\beta\alpha}$. The cross section is defined as the transition rate times photon energy divided by the intensity:

$$\sigma_{\beta\alpha} = \frac{W_{\beta\alpha}\hbar\omega_{\beta\alpha}}{I(\omega_{\beta\alpha})}\,, \tag{5.20}$$

The intensity of an electric field can be written $I(\omega_{\beta\alpha}) = \frac{1}{2}\epsilon_0 c E_0^2(\omega)$. Taking the constants out of the squared matrix element and expressing the matrix element as:

$$M_{\beta\alpha} = \langle\psi_\beta|\mathbf{r}|\psi_\alpha\rangle\,, \tag{5.21}$$

yields the following expression for cross section:

$$\sigma_{\beta\alpha} = \frac{e^2\pi\omega_{\beta\alpha}}{\epsilon_0 c}|M_{\beta\alpha}|^2\rho(E_\beta)\,. \tag{5.22}$$

Substituting in the fine structure constant $\alpha = \frac{e^2}{4\pi\epsilon_0\hbar c}$ gives the final expression for photoionization cross section:

$$\sigma_{\beta\alpha} = 4\pi^2\alpha\hbar\omega_{\beta\alpha}|M_{\beta\alpha}|^2\rho(E_\beta)\,. \tag{5.23}$$

Our wave functions can be described by their set of quantum numbers:

$$|\psi\rangle = |k\, j\, m_j,\, l\, s\rangle\,. \tag{5.24}$$

The transitions under study are from $\alpha = 1s$ to $\beta = kp$. For these transitions we have: $l' = 0$, $l = 1$ and $s' = s = \frac{1}{2}$. The spin being known gives only two possible values for j

$$j_+ = l + \frac{1}{2} = \frac{3}{2}, \qquad j_- = \left|l - \frac{1}{2}\right| = \frac{1}{2}\,. \tag{5.25}$$

For the combinations of quantum numbers we shall assume the magnetic quantum number to be $m_l = 0$ and that the spin quantum number is $m_s = +\frac{1}{2}$, both before and after the interaction. The possible value for the projection of the total angular momentum quantum number $m_j = m_l + m_s$ is now $m_j = \frac{1}{2}$. Since we have fixed our system to $m_s = \frac{1}{2}$ we can picture that in the two cases of different j, orbital angular momentum and spin vectors are either parallel or anti-parallel. The matrix elements for interactions between $1s$ and kp states become:

$$M^{j+}_{kp,1s} = \left\langle k\,\frac{3}{2}\,\frac{1}{2},\, 1\,\frac{1}{2}\,\middle|\,\mathbf{r}\,\middle|\,1\,\frac{1}{2}\,\frac{1}{2}\,,0\,\frac{1}{2}\right\rangle \tag{5.26}$$

$$M^{j-}_{kp,1s} = \left\langle k\,\frac{1}{2}\,\frac{1}{2}\,,\, 1\,\frac{1}{2}\,\middle|\,\mathbf{r}\,\middle|\,1\,\frac{1}{2}\,\frac{1}{2}\,,\,0\,\frac{1}{2}\right\rangle. \tag{5.27}$$

Writing our states in the coupled picture; the Clebsch-Gordan coefficients have been included in the final states when computing the matrix elements from (5.26) and (5.27). The coefficients for the case $j_+ = \frac{3}{2}$ and $j_- = \frac{1}{2}$, respectively are given by [20]:

$$C_+ = \sqrt{\frac{l + \frac{1}{2} + m_j}{2l+1}} = \sqrt{\frac{2}{3}}\,, \tag{5.28}$$

$$C_- = -\sqrt{\frac{l + \frac{1}{2} - m_j}{2l+1}} = -\sqrt{\frac{1}{3}}\,. \tag{5.29}$$

The photon energy being $E_{kp} - E_{1s} = \hbar\omega_{kp,1s}$ and $\hbar = 1$ in atomic units, the implemented formula is:

$$\sigma_{kp,1s} = 4\pi^2 \alpha E_{kp,1s} \left| M^{j_\pm}_{kp,1s} \right|^2 \rho(E_{kp}) \,, \tag{5.30}$$

where the density of states is given by:

$$\rho(E_{kp}) = \frac{2}{E_{(k+1)p} - E_{(k-1)p}} \,. \tag{5.31}$$

5.2 Results and discussion

A study of the photoionization cross section for both the non-relativistic case and the relativistic case will be presented. To account for relativistic effects, relativistic correction terms in the Hamiltonian have been implemented. The two Hamiltonians applied in the calculations are:

$$\hat{H}_{nonrel} = \frac{\hat{p}^2}{2m} + V(r) + e\mathbf{E}(t) \cdot \mathbf{r} \,, \tag{5.32}$$

$$\hat{H}_{rel} = \frac{\hat{p}^2}{2m} + V(r) - \frac{\hat{p}^4}{8m^3c^2} + \frac{e^2}{8\pi\epsilon_0} \frac{1}{m^2c^2r^3} \hat{\mathbf{L}} \cdot \hat{\mathbf{S}} + \frac{\pi\hbar^2}{2m^2c^2} \frac{e^2}{4\pi\epsilon_0} \delta(\mathbf{r}) + e\mathbf{E}(t) \cdot \mathbf{r} \tag{5.33}$$

The following questions are attempted answered:

- **Can relativistic effects be observed for the photoionization cross section?**
- **Do cross section results obtained from solving the Dirac equation agree with results obtained from the Schrödinger equation with relativistic corrections?**
- **Will the orientation of the spin and angular momentum have an effect on the cross section?**

A basis of ≈ 1400 splines in a box of size $r_{max} = 30$ a.u. were used for this calculation. Of the 1400 eigenstates $N_{max} = 900$ were kept. Using these parameters we will show results for energies up to $E = 2500$ a.u. The unit of cross section is megabarn, $1\text{Mb} = 10^{-18}\text{cm}^2$, a unit much used in nuclear physics.

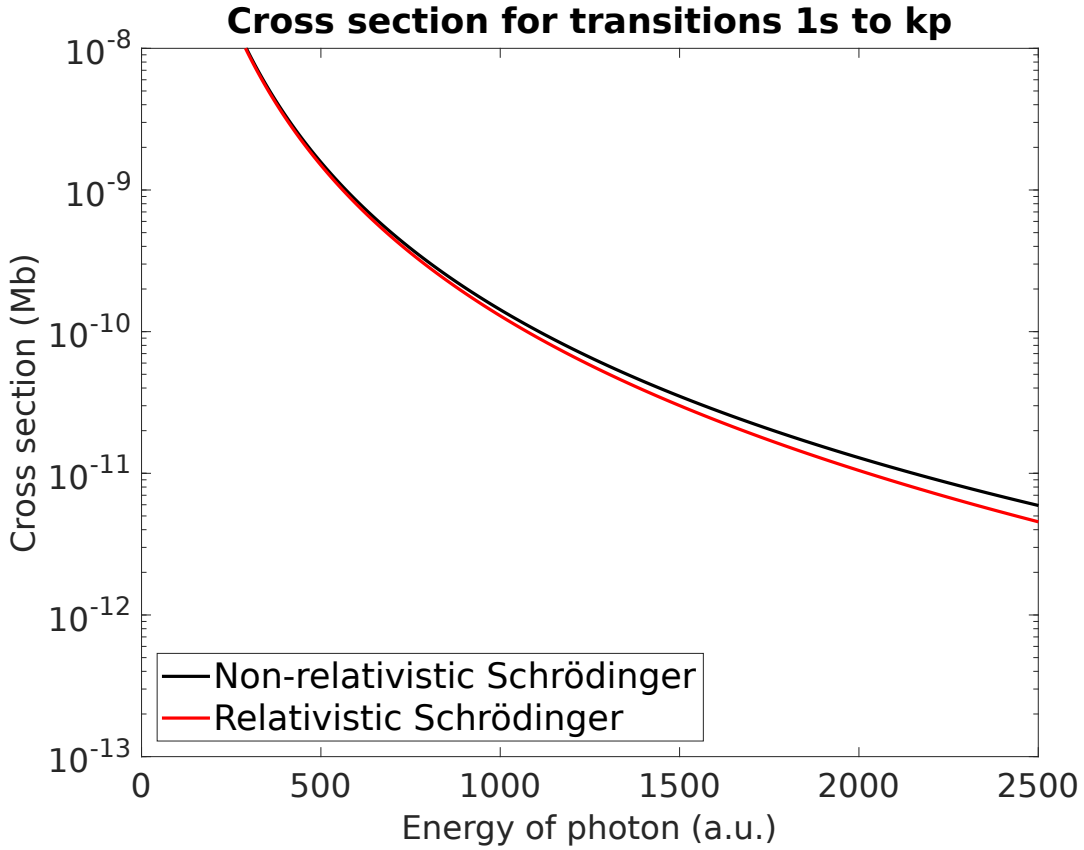

Figure 5.1: The figure shows photoionization cross section with respect to photon energy. Unit of cross section is in megabarn, where 1 Mb = 10^{-18}cm^2. The solid black line represents the calculation using the Hamiltonian (5.32) for the non-relativistic system. The red solid line shows the calculation using the Hamiltonian (5.33) for the relativistic system. It can be observed that the relativistic effects cause the cross section to be smaller than for the non-relativistic system.

First, the photoionization cross section for the non-relativistic case is presented and compared to the relativistic case. Both calculations are performed using the Schrödinger equation using the Hamiltonians (5.32) and (5.33). Figure (5.1) shows the calculation using the non-relativistic Hamiltonian (5.32) represented by the black line. The red line shows the relativistic calculation using the Hamiltonian (5.33). Generally, the cross section decreases with increasing energy of the incoming photon. The cross section being proportional to the transition rate, $W_{\beta\alpha}$ (5.20), indicates that the probability of ionization will decrease with photon energy as well. Relativistic effects can be noticed from photon energies of about 1000 a.u., which is about 27.2 keV, and the effect becomes more distinguished with increasing photon energy. The effect manifests itself in that it gives a smaller cross section than for the non-relativistic calculation.

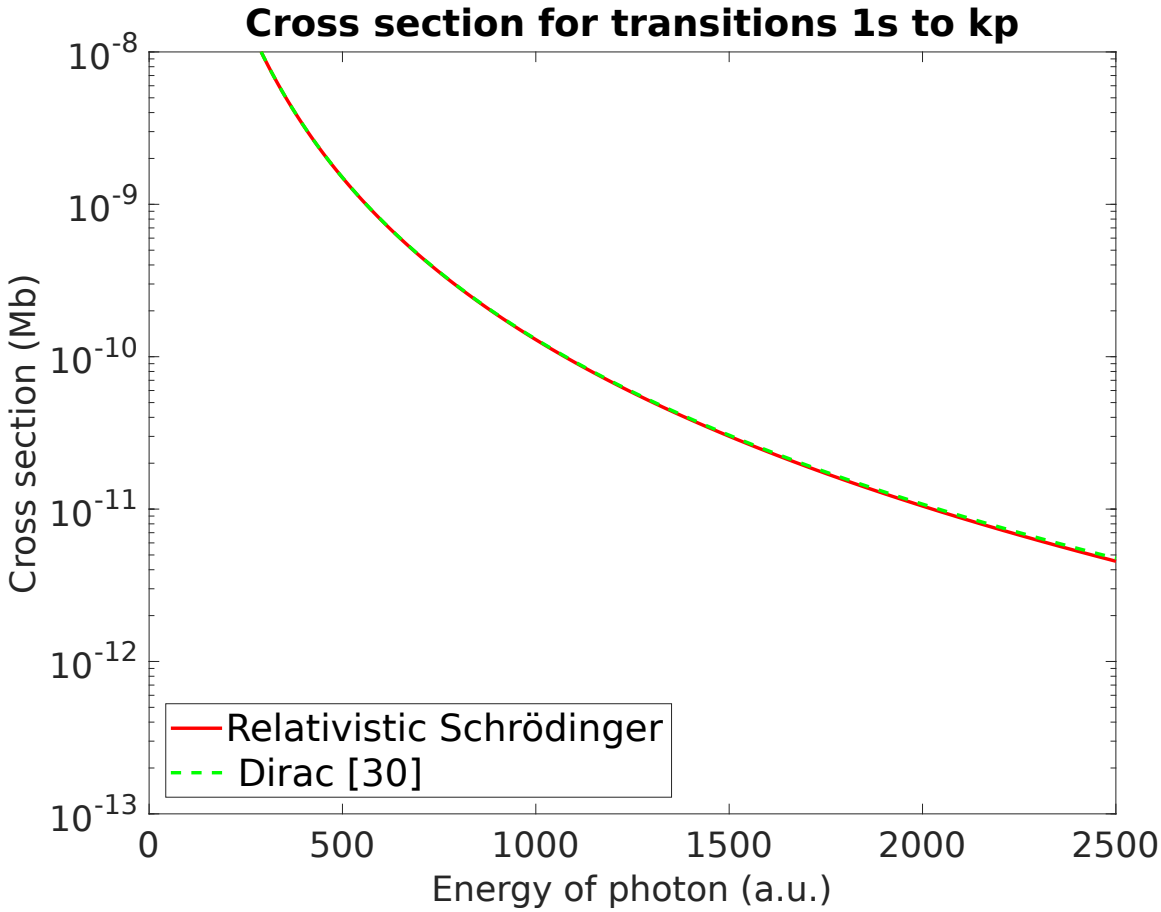

Figure 5.2: The red solid line is the same relativistic Schrödinger photoionization cross section calculation from the previous figure (5.1). Overlapping the red line is the green dashed line representing the Dirac equation calculation for cross section. The Dirac data were obtained from [30]. The two sets of results overlap nicely until we reach energies of 1500 a.u. and higher, then a small difference can be noticed.

Figure (5.2) presents the relativistic photoionization cross section solved by the Schrödinger equation, using the relativistic Hamiltonian (5.33), and the Dirac equation. Dirac equation results have been obtained from [30]. The two approaches yield very similar results, although a difference is observable at photon energies of 1500 a.u. and higher. The difference is nevertheless small and there seem to be good agreement between the relativistic Schrödinger equation approach and the Dirac equation approach.

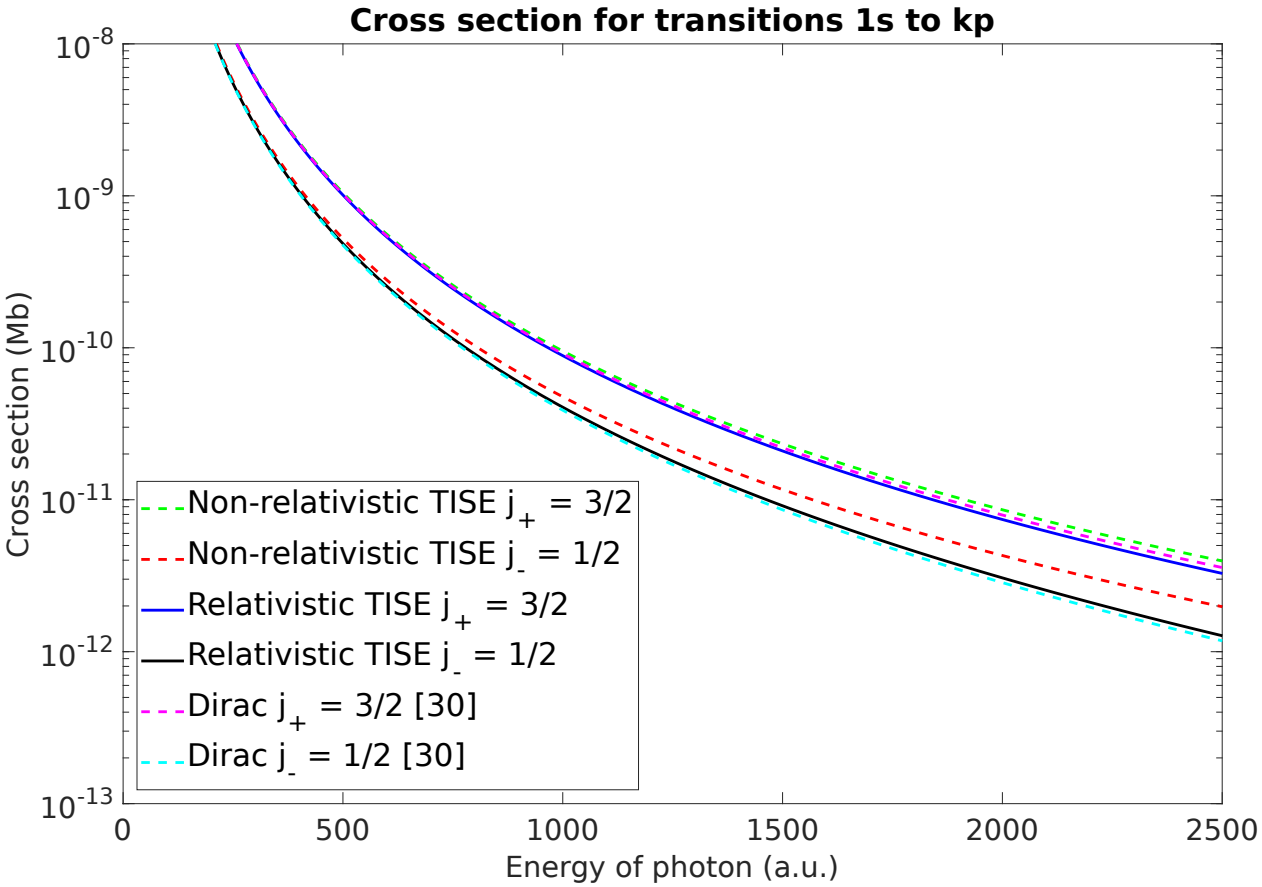

Figure 5.3: The solid lines represent cross section calculations from the Schrödinger equation using the relativistic Hamiltonian (5.33) and the dashed cyan and magenta lines represent calculations from the Dirac equation (obtained from [30]). Dashed lines in the colors green and red are the non-relativistic Schrödinger equation calculations using the Hamiltonian (5.32). Cross section for the two different values of j, the total angular momentum, have been separated. For the relativistic results their sum equal the curves in the previous figure, (5.2). Figure (5.1) show the sum of the non-relativistic results by its black solid line. The dashed green and magenta line, together with the solid blue line all show cases where the electron's final state has parallel spin and angular momentum, $j_+ = 3/2$. For the three remaining lines: the red and cyan dashed lines and the black solid line, they all show cases where the spin and angular momentum are anti-parallel, j_-, for the electron in the final state.

Figure (5.3) shows the separation of the cases with parallel, $j_+ = \frac{3}{2}$, and anti-parallel, $j_- = \frac{1}{2}$, angular momentum and spin. The solid lines show the photoionization cross section calculated using the Schrödinger equation where the relativistic Hamiltonian (5.33) has been implemented. For these calculations the matrix elements of the interaction are given by (5.26) and the cross section is represented by the blue solid line for the parallel case. Similarly for the anti-parallel case; the matrix elements are given by (5.27) and the cross section is depicted by the black solid line. Represented by the dashed lines are the photoionization cross section results from the Dirac equation and the non-relativistic Schrödinger equation. $j_+ = \frac{3}{2}$ is shown in figure (5.3) by the dashed magenta line for Dirac and by the dashed green line for non-relativistic Schrödinger. $j_- = \frac{1}{2}$ is represented by

the dashed cyan line for Dirac and by the dashed red line for non-relativistic Schrödinger. The sum of the blue and black solid lines yield the solid red curve in figure (5.2) and the sum of the dashed magenta and cyan lines yield the dashed green curve in figure (5.2). Lastly, the sum of the dashed green and red line yields the black solid curve in (5.1)

From figure (5.3) a profound difference between j_+ and j_- is observable. As a consequence of the Clebsch-Gordan coefficients (5.28) and (5.29) there is generally a smaller probability for an electron to end up with anti-parallel spin and angular momentum. It can thus be seen that the j_- calculation yields a smaller cross section than the j_+ case with parallel spin and angular momentum. From photon energies of 500 a.u. and higher a difference between the Dirac and the relativistic Schrödinger results can be observed. For the j_+ case in figure (5.3) the Dirac result is generally a little higher when compared to the relativistic Schrödinger calculation. For the j_- case the Dirac result is generally a little lower. This leaves the apparent agreement of the result in figure (5.2) somewhat debatable. Since the difference between the non-relativistic Schrödinger calculation and the Dirac calculation is of the same magnitude as the difference between the Dirac and relativistic Schrödinger equation for the j_+ case a further investigation of these effects is necessary to draw any conclusions. It is not certain why we get these differences between the Dirac and the relativistic Schrödinger equation but possible sources are errors in the programming or effects from other correction terms such as the second order correction to the kinetic energy:

$$\frac{p^6}{16m^5c^4}\,. \tag{5.34}$$

Although it must be noticed that this term is proportional to α^4 and thus is very small, it leaves a possibility for further investigation. As the dipole approximation has shown to break down for high photon energies, performing the calculation including beyond dipole effects is also an option for further exploration.

Chapter 6

Multiphoton Ionization of Hydrogen - a Time Dependent Study

A study of ionization of the hydrogen atom will now be presented. The hydrogen atom is exposed to an intense laser field and the probability of ionization will be studied for both the non-relativistic case and when we consider relativistic effects in the calculations. Plots showing the differential probability of ionization will be shown, where results from the non-relativistic and relativistic Schrödinger equation will be compared to results from solving the Dirac equation as was calculated by [34].

To obtain these results we must solve the time dependent Schrödinger equation

$$i\hbar\frac{\partial}{\partial t}\Psi(t,\mathbf{r}) = \hat{H}\Psi(t,\mathbf{r}) \tag{6.1}$$

numerically. Truncating the wave function at a number of states N_{max} per angular momentum states l, up to l_{max}, gives the following expression for the wave function:

$$\Psi(\mathbf{r},t) = \sum_{k=1}^{N_{max}}\sum_{l=0}^{l_{max}} c_{kl}(t)\psi_{kl}(\mathbf{r})\,. \tag{6.2}$$

Multiplying by $\Psi^*(\mathbf{r},t)$ from the left in equation (6.1) and taking the integral over all of space yields an only time dependent set of differential equations, which we can solve as a matrix equation:

$$i\hbar\begin{bmatrix}\dot{c}_1(t)\\ \dot{c}_2(t)\\ \vdots\\ \dot{c}_q(t)\end{bmatrix} = \begin{bmatrix}H_{11} & H_{12} & \dots & H_{1q}\\ H_{21} & H_{22} & \dots & H_{2q}\\ \vdots & \vdots & \ddots & \vdots\\ H_{p1} & \dots & \dots & H_{pq}\end{bmatrix}\begin{bmatrix}c_1(t)\\ c_2(t)\\ \vdots\\ c_q(t)\end{bmatrix}. \tag{6.3}$$

The matrix elements of the Hamiltonian is computed before the Hamiltonian can be propagated forward in time. The time propagation is performed using a Fortran program based on a numerical method from [31].

6.1 Calculating the matrix elements of the velocity gauge Hamiltonian

Computing the matrix elements of the Hamiltonian in (6.3) is an arduous task. We want to solve the problem for intense laser fields, where the photoelectron reaches relativistic velocities, therefore we shall consider the velocity gauge Hamiltonian (3.14) from chapter 3. It has been shown that when solving the time-dependent Schrödinger equation for intense fields the velocity gauge proves more efficient than the length gauge [32, 33]. Quantum mechanics is gauge invariant, but the two gauges present different computational properties. A higher l_{max} is required for calculations in length gauge; it is therefore more convenient to apply the velocity gauge Hamiltonian for this task.

The non-relativistic Hamiltonian is then the Hamiltonian (3.19) from chapter 3.

$$\hat{H}_{nonrel} = \frac{\hat{p}^2}{2m} + \frac{e(\mathbf{A}\cdot\hat{\mathbf{p}})}{m} + V(r)\,, \tag{6.4}$$

Expanding the parentheses for the relativistic velocity gauge Hamiltonian (3.14) gives the following extensive expression:

$$\begin{aligned}\hat{H}_{rel} = &-\frac{\hat{p}^2}{2m} - \frac{e^2}{4\pi\epsilon_0 r} + \frac{e\hat{p}_z\mathbf{A}}{m} + \frac{e^2\mathbf{A}^2}{2m} - \frac{\hat{p}^4}{8m^3c^2} - \frac{e\hat{p}^2\hat{p}_z\mathbf{A}}{2m^3c^2} \\ &-\frac{1}{4}\frac{e^2\hat{p}^2\mathbf{A}^2}{m^3c^2} - \frac{e^2(\hat{p}_z\cdot\mathbf{A})(\hat{p}_z\cdot\mathbf{A})}{2m^3c^2} - \frac{e^3\hat{p}_z\mathbf{A}^3}{2m^3c^2} - \frac{e^4\mathbf{A}^4}{8m^3c^2} \\ &+\frac{e^2}{8\pi\epsilon_0}\frac{1}{m^2c^2r^3}\big(\mathbf{r}\times(\hat{\mathbf{p}}+e\mathbf{A})\big)\cdot\hat{\mathbf{S}} + \frac{\pi\hbar^2}{2m^2c^2}\frac{e^2}{4\pi\epsilon_0}\delta(\mathbf{r})\end{aligned} \tag{6.5}$$

In the discussion about the dipole approximation in chapter 3 we performed a gauge transformation on the wave function (3.18) that caused the diamagnetic term $\frac{e^2\mathbf{A}^2}{2m}$ to disappear. For similar reasons the term $\frac{e^4\mathbf{A}^4}{8m^3c^2}$ also disappears. For an intense field the field strength is high and the terms proportional to high orders of $\mathbf{A}$ become important. We assume therefore that the LS-coupling and Darwin term can be neglected in the calculation. The LS-coupling is proportional to the field of the first order and the Darwin term is only a structural correction. The Hamiltonian used for calculations is now:

$$\begin{aligned}\hat{H}^{calc}_{rel} = &-\frac{\hat{p}^2}{2m} - \frac{e^2}{4\pi\epsilon_0 r} + \frac{e\hat{p}_z\mathbf{A}}{m} - \frac{\hat{p}^4}{8m^3c^2} - \frac{e\hat{p}^2\hat{p}_z\mathbf{A}}{2m^3c^2} \\ &-\frac{1}{4}\frac{e^2\hat{p}^2\mathbf{A}^2}{m^3c^2} - \frac{e^2(\hat{p}_z\cdot\mathbf{A})(\hat{p}_z\cdot\mathbf{A})}{2m^3c^2} - \frac{e^3\hat{p}_z\mathbf{A}^3}{2m^3c^2}\,.\end{aligned} \tag{6.6}$$

The calculation of the matrix elements of the 5 remaining field dependent terms will be shown. The coupling of the field with the momentum will be set aside for now and the spatial Hamiltonian will be calculated, considering only the z-component of the momentum. All the remaining terms contain only the hermitian operators $\hat{p}^2$ and $\hat{p}_z$. When these operators work on our wave function $\psi(\mathbf{r}) = \frac{\mathcal{U}_{kl}}{r}Y_{lm}$ they yield:

$$\hat{p}_z\psi(\mathbf{r}) = -i\hbar\frac{\partial}{\partial z}\left(\frac{\mathcal{U}_{kl}(r)}{r}Y_{lm}(\theta,\phi)\right) =$$
$$-i\left(\left(\frac{1}{r}\frac{d\mathcal{U}_{kl}}{dr} - \frac{l+1}{r^2}\mathcal{U}_{kl}\right)b_{l+1,m}Y_{l+1,m} + \left(\frac{1}{r}\frac{d\mathcal{U}_{kl}}{dr} + \frac{l}{r^2}\mathcal{U}_{kl}\right)b_{lm}Y_{l-1,m}\right) \tag{6.7}$$

$$\hat{p}^2\psi(\mathbf{r}) = -\hbar^2\nabla^2\left(\frac{\mathcal{U}_{kl}(r)}{r}Y_{lm}(\theta,\phi)\right) =$$
$$-\hbar^2\left(\frac{1}{r}\frac{d^2\mathcal{U}_{kl}}{dr^2}Y_{lm} - \frac{l(l+1)}{r^3}\mathcal{U}_{kl}Y_{lm}\right). \tag{6.8}$$

The b_{lm} factors are the Clebsch-Gordan coefficients. They are calculated using the relation:

$$b_{lm} = \sqrt{\frac{l^2-m^2}{(4l^2-1)}} \tag{6.9}$$

where $m = 0$.

The terms:

$$\hat{H}^{p_z} = \frac{\hat{p}_z\cdot e\mathbf{A}}{m} \qquad \text{and} \qquad \hat{H}^{p_zA^3} = -\frac{e^3\hat{p}_z\mathbf{A}^3}{2m^3c^2} \tag{6.10}$$

of the Hamiltonian (6.6) both operate like (6.7). They yield the following integrals for their matrix elements, respectively:

$$H^{p_z}_{pq} = -\frac{ie\hbar}{m}b_{l+1,m}\delta_{l',l+1}\delta_{mm'}\int_0^{r_{max}}\mathcal{U}_{kl}\frac{d\mathcal{U}_{k'l+1}}{dr} + \frac{l+1}{r}\mathcal{U}_{kl}\mathcal{U}_{k'l+1}dr\,, \tag{6.11}$$

$$H^{p_zA^3}_{pq} = \frac{ie^3\hbar}{2m^3c^2}b_{l+1,m}\delta_{l',l+1}\delta_{mm'}\int_0^{r_{max}}\mathcal{U}_{kl}\frac{\mathcal{U}_{k'l+1}}{dr} + \frac{l+1}{r}\mathcal{U}_{kl}\,\mathcal{U}_{k'l+1}\,dr\,, \tag{6.12}$$

when only taking into account the terms that satisfy $l' = l+1$. The matrix is symmetric so there is no need to calculate the same elements twice. The Jacobien r^2 have been included in all the integrals since we are working with spherical coordinates. For the term $\propto \hat{p}^2\hat{p}_z$ of (6.6),

$$\hat{H}^{p^2p_z} = -\frac{e\hat{p}^2\hat{p}_z\mathbf{A}}{2m^3c^2}\,, \tag{6.13}$$

we operate from both left and right. Operating with p^2 from the left and p_z from the right gives the following integral for the matrix elements:

$$H^{p^2p_z}_{pq} = -\frac{ie\hbar^3}{2m^3c^2}b_{l+1,m}\delta_{l',l+1}\delta_{mm'}\int_0^{r_{max}}\frac{d^2\mathcal{U}_{kl}}{dr^2}\frac{d\mathcal{U}_{k'l+1}}{dr} + \frac{l+1}{r}\frac{d^2\mathcal{U}_{kl}}{dr^2}\mathcal{U}_{k'l+1}$$
$$-\frac{l(l+1)}{r^2}\frac{d\mathcal{U}_{k'l+1}}{dr}\mathcal{U}_{kl} - \frac{l(l+1)^2}{r^3}\mathcal{U}_{k',l+1}\mathcal{U}_{kl}\,dr\,. \tag{6.14}$$

The term

$$\hat{H}^{p^2} = -\frac{e^2\hat{p}^2\mathbf{A}^2}{4m^3c^2} \tag{6.15}$$

in (6.6) yields the following integral for its matrix elements:

$$H^{p^2}_{pq} = -\frac{e^2\hbar^2}{4m^3c^2}\delta_{ll'}\delta_{mm'}\int_0^{r_{max}} \frac{d^2\mathcal{U}_{k'l}}{dr^2}\mathcal{U}_{kl} - \frac{l(l+1)}{r^2}\mathcal{U}_{kl}\,\mathcal{U}_{k'l}\,dr\,. \tag{6.16}$$

Lastly, the term

$$\hat{H}^{p_zp_z} = -\frac{e^2(\hat{p}_z\cdot\mathbf{A})(\hat{p}_z\cdot\mathbf{A})}{2m^3c^2} \tag{6.17}$$

of the Hamiltonian (6.6) requires us to operate with $\hat{p}_z$ twice so here we will also work from both right and left. Working with $\hat{p}_z$ from the left means we must take the complex conjugate on the momentum operator; changing it from $-i\hbar\frac{\partial}{\partial z}$ to $+i\hbar\frac{\partial}{\partial z}$. These matrix elements are the most extensive to calculate; coupling both states of $l' = l$ and also $l' = l+2$.

$$\begin{aligned}
H^{p_zp_z}_{pq} = -\frac{e^2\hbar^2}{2m^3c^2}\Bigg(& b_{l+1,m}b_{l'+1,m'}\delta_{ll'}\delta_{mm'}\int_0^{r_{max}}\Bigg(\frac{d\mathcal{U}_{kl}}{dr}\frac{d\mathcal{U}_{k'l}}{dr} - \frac{l+1}{r}\frac{d\mathcal{U}_{kl}}{dr}\mathcal{U}_{k'l} \\
&- \frac{l+1}{r}\frac{d\mathcal{U}_{k'l}}{dr}\mathcal{U}_{kl} + \frac{(l+1)^2}{r^2}\mathcal{U}_{kl}\,\mathcal{U}_{k'l}\Bigg)\,dr \\
&+ b_{l,m}b_{l',m'}\delta_{ll'}\delta_{mm'}\int_0^{r_{max}}\Bigg(\frac{d\mathcal{U}_{kl}}{dr}\frac{\mathcal{U}_{k'l}}{dr} + \frac{l}{r}\frac{d\mathcal{U}_{kl}}{dr}\mathcal{U}_{k'l} \\
&+ \frac{l}{r}\frac{d\mathcal{U}_{k'l}}{dr}\mathcal{U}_{kl} + \frac{l^2}{r^2}\mathcal{U}_{kl}\,\mathcal{U}_{k'l}\Bigg)\,dr \\
&+ b_{l+1,m}b_{l+2,m'}\delta_{l,l+2}\delta_{mm'}\int_0^{r_{max}}\Bigg(\frac{d\mathcal{U}_{kl}}{dr}\frac{d\mathcal{U}_{k'l+2}}{dr} + \frac{l+2}{r}\frac{d\mathcal{U}_{kl}}{dr}\mathcal{U}_{k'l+2} \\
&- \frac{l+1}{r}\frac{d\mathcal{U}_{k'l+2}}{dr}\mathcal{U}_{kl} - \frac{(l+1)(l+2)}{r^2}\mathcal{U}_{kl}\,\mathcal{U}_{k'l+2}\Bigg)\,dr\Bigg)
\end{aligned} \tag{6.18}$$

All the integrals are calculated using the Gauss-Legendre integration method. The total Hamiltonian matrix is relatively sparse: it forms a coordinate system where horizontally in the matrix we increase the integer value of l' and downwards vertically we increase the integer value of l. For each combination of quantum numbers l' and l there is a $N_l \times N_l$ submatrix within the Hamiltonian, which is apparent in the subscript of the factor $\delta_{ll'}$. From $H^{p_z}_{pq}$ (6.11),$H^{p_zA^3}_{pq}$ (6.12) and $H^{p^2p_z}_{pq}$ (6.14) we get elements placed in the submatrices where $l' = l+1$, and $l' = l-1$. The elements from the first two integrals of H^{pzpz}_{pq} (6.18) are placed together with elements from $H^{p^2}_{pq}$ (6.16) in submatrices along the diagonal

where $l = l'$ is satisfied. The remaining elements from the third integral of H_{pq}^{pzpz} (6.18) have the condition $l' = l + 2$ and $l' = l - 2$.

Below we show the structure of a Hamiltonian matrix for the case $l_{max} = l'_{max} = 7$. Inside each $N_l \times N_l$ submatrix the corresponding quantum number l and l' is stated. Since no integrals give non-zero values beyond $l' = l + 2$ or below $l' = l - 2$ the matrix gets a diagonal stripe of width $5 \cdot N_l$ non-zero elements:

$$\begin{bmatrix}
\begin{bmatrix} l=0 \\ l'=0 \end{bmatrix} & \begin{bmatrix} l=0 \\ l'=1 \end{bmatrix} & \begin{bmatrix} l=0 \\ l'=2 \end{bmatrix} & & & & & & \\
\begin{bmatrix} l=1 \\ l'=0 \end{bmatrix} & \begin{bmatrix} l=1 \\ l'=1 \end{bmatrix} & \begin{bmatrix} l=1 \\ l'=2 \end{bmatrix} & \begin{bmatrix} l=1 \\ l'=3 \end{bmatrix} & & & & \mathbf{0} & \\
\begin{bmatrix} l=2 \\ l'=0 \end{bmatrix} & \begin{bmatrix} l=2 \\ l'=1 \end{bmatrix} & \begin{bmatrix} l=2 \\ l'=2 \end{bmatrix} & \begin{bmatrix} l=2 \\ l'=3 \end{bmatrix} & \begin{bmatrix} l=2 \\ l'=4 \end{bmatrix} & & & & \\
 & \begin{bmatrix} l=3 \\ l'=1 \end{bmatrix} & \begin{bmatrix} l=3 \\ l'=2 \end{bmatrix} & \begin{bmatrix} l=3 \\ l'=3 \end{bmatrix} & \begin{bmatrix} l=3 \\ l'=4 \end{bmatrix} & \begin{bmatrix} l=3 \\ l'=5 \end{bmatrix} & & & \\
 & & \begin{bmatrix} l=4 \\ l'=2 \end{bmatrix} & \begin{bmatrix} l=4 \\ l'=3 \end{bmatrix} & \begin{bmatrix} l=4 \\ l'=4 \end{bmatrix} & \begin{bmatrix} l=4 \\ l'=5 \end{bmatrix} & \begin{bmatrix} l=4 \\ l'=6 \end{bmatrix} & & \\
 & & & \begin{bmatrix} l=5 \\ l'=3 \end{bmatrix} & \begin{bmatrix} l=5 \\ l'=4 \end{bmatrix} & \begin{bmatrix} l=5 \\ l'=5 \end{bmatrix} & \begin{bmatrix} l=5 \\ l'=6 \end{bmatrix} & \begin{bmatrix} l=5 \\ l'=7 \end{bmatrix} & \\
 & \mathbf{0} & & & \begin{bmatrix} l=6 \\ l'=4 \end{bmatrix} & \begin{bmatrix} l=6 \\ l'=5 \end{bmatrix} & \begin{bmatrix} l=6 \\ l'=6 \end{bmatrix} & \begin{bmatrix} l=6 \\ l'=7 \end{bmatrix} & \\
 & & & & & \begin{bmatrix} l=7 \\ l'=5 \end{bmatrix} & \begin{bmatrix} l=7 \\ l'=6 \end{bmatrix} & \begin{bmatrix} l=7 \\ l'=7 \end{bmatrix} &
\end{bmatrix}$$

6.2 Describing the electromagnetic field

The vector potential describes our electromagnetic field. It is originally both space and time dependent and can be written:

$$\mathbf{A}(\mathbf{r}, t) = A_0(\omega)\hat{\boldsymbol{\epsilon}} f(\mathbf{r}, t) \cos(\mathbf{k} \cdot \mathbf{r} - \omega t + \delta) \tag{6.19}$$

where A_0 is the amplitude of the field and $\hat{\boldsymbol{\epsilon}}$ is the unit vector pointing in the direction of polarization. $\mathbf{k}$ is the wave vector pointing in the direction of propagation. If the direction of propagation is perpendicular to the polarization direction $\mathbf{k} \cdot \hat{\boldsymbol{\epsilon}} = 0$ then the waves are transverse. ω is the angular frequency, δ is the phase and the function $f(\mathbf{k} \cdot \mathbf{r} - \omega t)$ is the so-called envelope function, determining the shape of the field. The cosine term is called the carrier term and it describes the oscillations within the pulse.

We are choosing the polarization direction as the z direction and the propagation direction to be in the x direction. The propagation direction is perpendicular to the polarization direction so that the wave is transverse. Adopting the dipole approximation that was discussed in chapter 3 and neglecting the space dependence of the field yields:

$$\mathbf{A}(\mathbf{r}, t) \to \mathbf{A}(t) = A_0(\omega)\hat{\mathbf{z}} f(\omega t) \cos(\omega t + \delta)\,. \tag{6.20}$$

The envelope function is expressed as $f(\omega t) = \sin^2\left(\frac{\pi t}{T_{pulse}}\right)$. The duration of the pulse is determined by the frequency and the number of cycles from the relation $T_{pulse} = \frac{N \cdot 2\pi}{\omega}$. The amplitude is $A_0 = \frac{E_0}{\omega}$ where E_0 is the strength of the electric field

$$\mathbf{A}(t) = \frac{E_0}{\omega}\hat{\mathbf{z}}\sin^2\left(\frac{\pi t}{T_{pulse}}\right)\cos(\omega t + \delta)\,. \tag{6.21}$$

As the field is z-polarized it interacts only with the z-component of the momentum in minimal coupling. A frequency of $\omega = 50$ a.u. and $N = 15$ cycles have been applied for all calculations in this thesis. The phase shift ϕ between the envelope and the carrier has been set to 0. For a frequency of $\omega = 50$ a.u., the energy of the photons are 1360 eV.

6.3 Results and discussion

Our goal is to study the relativistic effects in photoionization of hydrogen. To reach this goal the TDSE using a velocity gauge Hamiltonian has been solved with and without relativistic corrections. The goals can be summarized in the following questions:

- **Does the Schrödinger equation, where relativistic corrections of first order have been included, produce results that coincide with results from the Dirac equation?**
- **Compared to the results from the non-relativistic Schrödinger equation how can relativistic effects be observed in ionization dynamics?**
- **Which of the relativistic correction terms are of importance?**

When the matrix equation (6.3) has been solved the values $|c_{kl}(T_{pulse})|^2$ give the probability of finding the electron in a state k for a quantum number l. The probability of finding the electron having energy E_k can be found by taking the sum over all l-states with probability of energy E_k after the duration of the pulse T_{pulse}

$$P(E_k) = \sum_l |c_{kl}(T_{pulse})|^2\,. \tag{6.22}$$

Imposing the condition that $E \leq 0$ gives us the probability for the electron to be in a bound state after the interaction. If we sum over all the probabilities when the energy is above zero we get the probability of the atom being ionized,

$$P_{ion} = P(E > 0) = \sum_{k=a}^{b}\sum_l |c_{kl}(T_{pulse})|^2\,. \tag{6.23}$$

where a and b are the first and last ionized states, respectively. The condition $E > 0$ imposed on the equation below gives us the differential probability for ionization with respect to energy:

$$\frac{dP}{dE} = P(E)\rho(E)\,. \tag{6.24}$$

Where $\rho(E)$ is the density of states:

$$\rho(E) = \frac{2}{E_{k+1} - E_{k-1}}\,. \tag{6.25}$$

Now that we know how to obtain the ionization probability we can move on to the time propagation results. Two different sets of parameters have been used for the basis. They

will be called the *small basis* and *large basis* for future reference and the parameters are listed in table (6.1). We will use both bases for our time dependent Schrödinger equation calculations and which basis is used will be specified in each case. Good convergence of the results for both basis sets were reached at $l_{max} = 14$. Variation of the parameters was performed until satisfactory convergence was reached. All B-splines are distributed equally over the box.

Parameter	Large	Small
r_{max}	65 a.u.	55 a.u.
l_{max}	14	14
N_{max}	710	485
E_{max}	580 a.u.	380 a.u.

Table 6.1: The parameters for the large basis and the small basis.

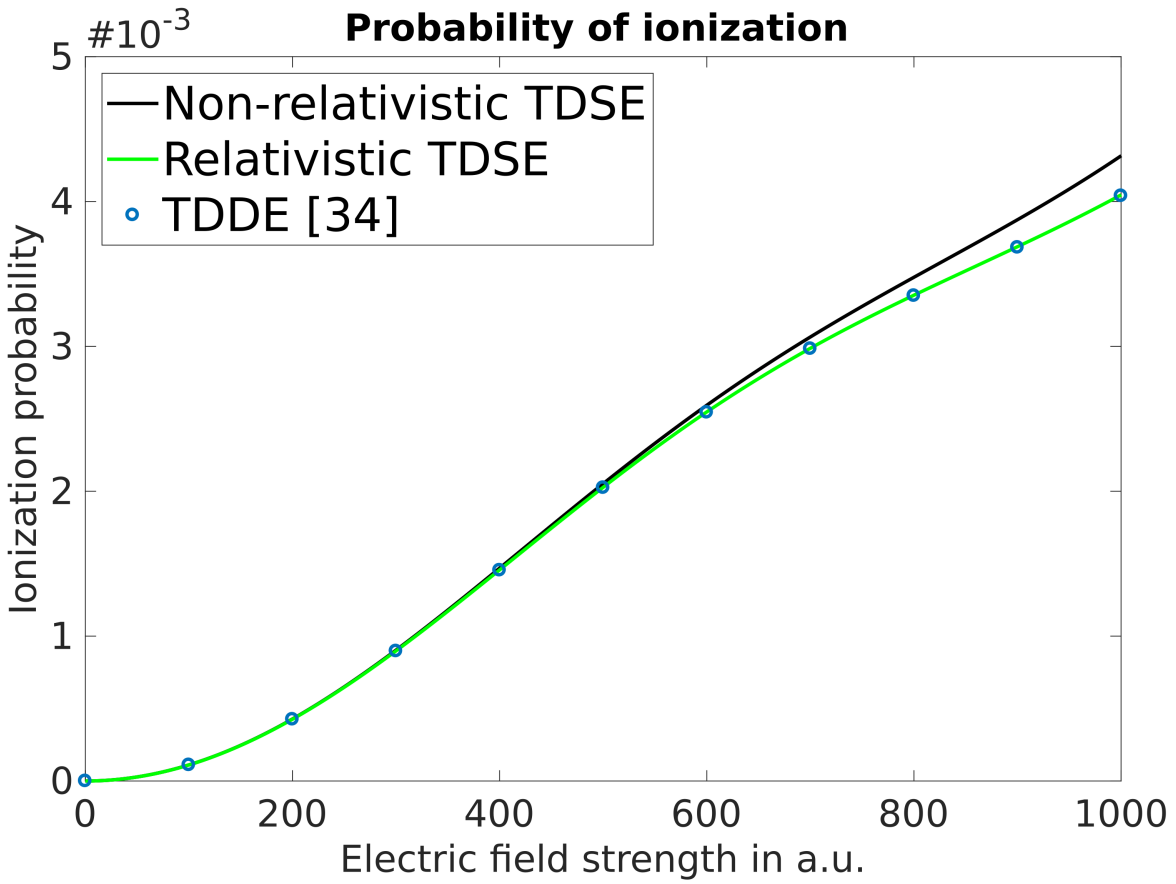

Figure 6.1: Ionization probability for hydrogen in a field of frequency $\omega = 50$ a.u. Relativistic and non-relativistic time dependent Schrödinger equation are represented by the solid green and black lines respectively. They are interpolations of points calculated with step size 50 a.u. for the electric field. The blue points show the results from the time dependent Dirac equation. The TDSE with relativistic corrections seem to agree with the results from the TDDE [34].

Figure 6.1 shows the ionization probability for absorption of one or more photons in the energy regime $0 < E < 380$. The TDSE has been solved using the non-relativistic Hamiltonian (6.4) depicted by the solid black line and the relativistic Hamiltonian (6.6) depicted by the solid green line. The curves are interpolations of calculated points for field strengths between 0 and 1000 with step size 50 for the TDSE. The large basis was used obtaining these results. The blue circles are the calculated points from the time dependent Dirac equation (TDDE). A stepsize of 100 has been used for the Dirac equation calculations and they were obtained from [34]. A basis corresponding to the small basis was used for calculation of the time dependent Dirac equation points.

Despite the difference in basis the results from the relativistic TDSE and the TDDE are in good agreement. For field strengths > 500 a.u. a lower ionization probability for the relativistic case is evident. This difference in probability of ionization has been observed by others before, for hydrogen [6, 10] and for helium(+) and boron(4+) [9].

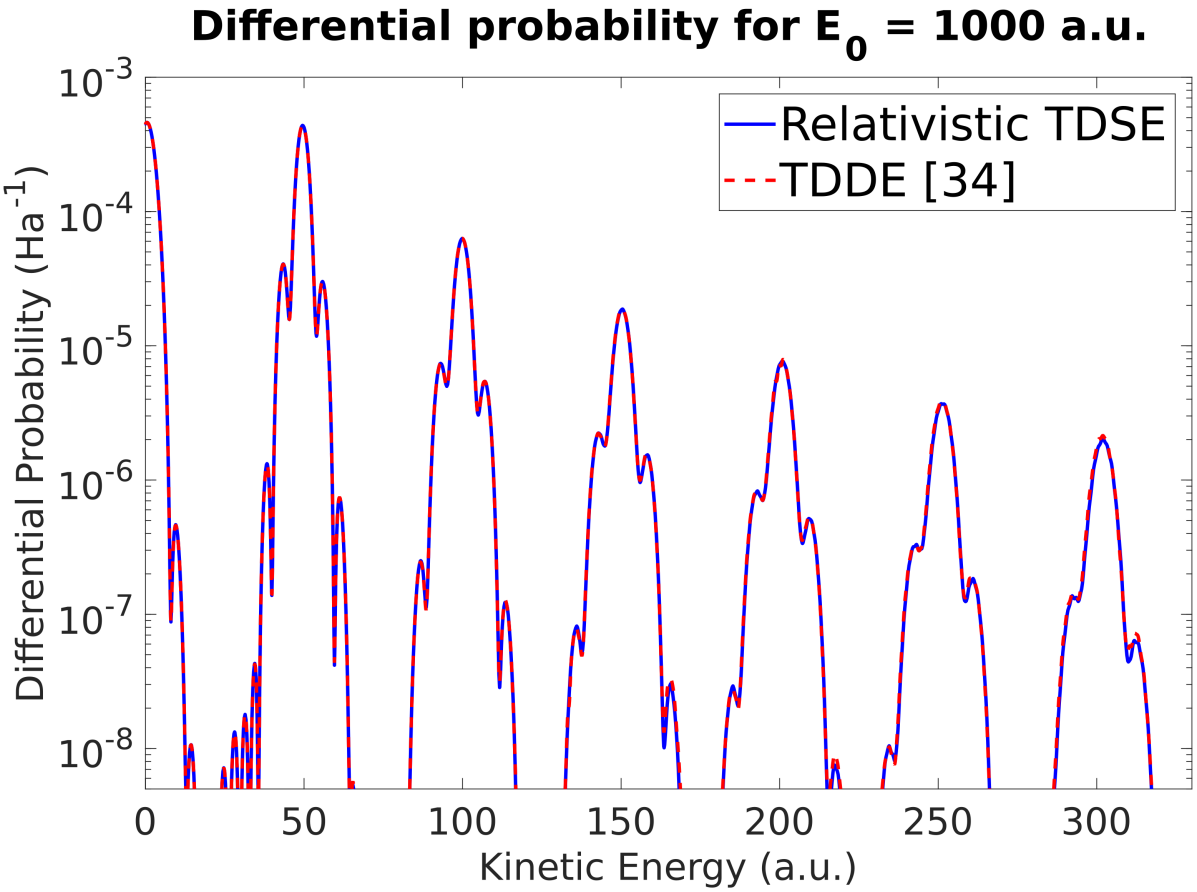

Figure 6.2: Comparison of the differential probability of ionization of hydrogen by simulations of the relativistic TDSE and the TDDE [34]. The intensity of the laser is $E_0 = 1000$ a.u. and the frequency is $\omega = 50$ a.u. Results from the relativistic Schrödinger equation using the Hamiltonian (6.6) are represented by the solid blue line and the red dashed line shows the results from the time dependent Dirac equation. Both TDSE and TDDE give the same probability density functions. Since the LS-coupling and the Darwin term are not considered in the TDSE calculation this is an indication that these terms are not important for the ionization dynamics.

Figure (6.2) shows the kinetic energy distribution of the photoelectron for the laser intensitiy $E_0 = 1000$. The solid blue line represents the calculation using the TDSE with the relativistic Hamiltonian (6.6). The dashed red line show the calculations from using the Dirac equation. Again, Dirac equation results were obtained from [34]. Both calculations were performed using the small basis. The two sets of results overlap nicely, indicating that solving the relativistic Schrödinger equation works as well as the Dirac equation in these cases. Even though the LS-coupling and Darwin term is not included in the Hamiltonian (6.6) the results from the TDSE and TDDE seem to agree. It can also be shown that excluding the $-\frac{\hat{p}^4}{8m^3c^2}$ term in the Hamiltonian (6.6) does not cause any displacement of the curve, which indicates that structural effects are not so important. The peaks of the curve are located in the vicinity of multiples of the photon energy $n \cdot \omega = n \cdot 50$, representing absorption of one or more photons.

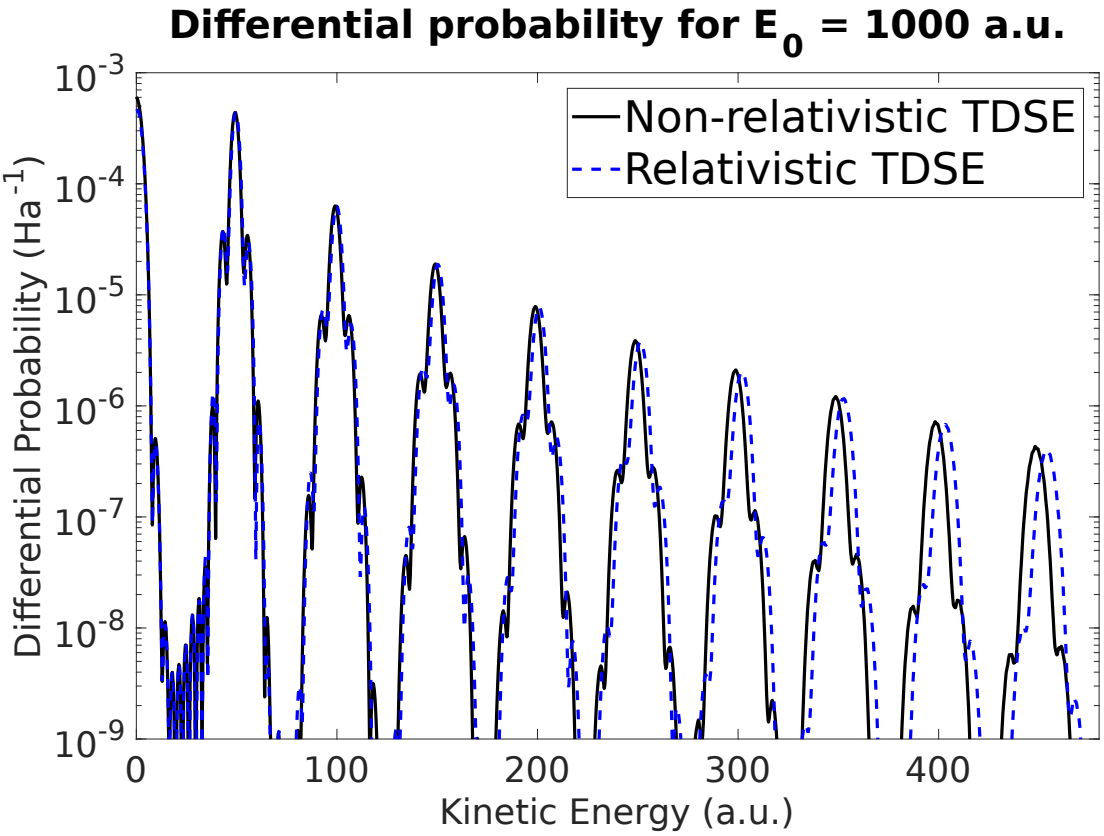

Figure 6.3: Non-relativistic TDSE probability density compared to results from the relativistic TDSE for laser intensity of $E_0 = 1000$ a.u. and frequency $\omega = 50$ a.u. The black solid curve shows the result from using the non-relativistic Hamilton (6.4). Results from the dashed blue line is using the Hamiltonian (6.6). The large basis is used for this calculation. The relativistic curve is shifted towards higher kinetic energies.

In figure (6.3) the black solid curve show the result from solving the non-relativistic TDSE with the Hamiltonian (6.4). Solving the TDSE with the Hamiltonian (6.6) gives the dashed blue line representing the relativistic calculation. The large basis has been used for these calculations allowing us to go to higher energies. Relativistic effects are pronounced in figure (6.3). Having already found that the Dirac equation and the relativistic Schrödinger equation give the same probability density we see that the relativistic calculations separate from the non-relativistic. As the photoelectron reaches kinetic energies of about 200 a.u. a displacement between the relativistic and non-relativistic curves becomes visible. The displacement is towards higher energies for the relativistic calculation. As more photons are absorbed the shift increases. This effect is probably due to the increased inertia of the electron as discussed in [10]. The momentum of a relativistic particle increases because of relativistic effects. And we see these effects in our results

$$\mathbf{p} = \frac{m\mathbf{v}}{\sqrt{1 - \frac{v^2}{c^2}}}\,. \tag{6.26}$$

Similar figures to figure (6.2) and (6.3) were produced where the interaction terms:

$$\frac{e\hat{p}^2\hat{p}_z\mathbf{A}}{2m^3c^2} - \frac{1}{4}\frac{e^2\hat{p}^2\mathbf{A}^2}{m^3c^2} - \frac{e^2(\hat{p}_z\cdot\mathbf{A})(\hat{p}_z\cdot\mathbf{A})}{2m^3c^2} - \frac{e^3\hat{p}_z\mathbf{A}^3}{2m^3c^2}\,, \tag{6.27}$$

were added to the Hamiltonian,

$$\hat{H} = -\frac{\hat{p}^2}{2m} - \frac{e^2}{4\pi\epsilon_0 r} + \frac{e\hat{p}_z\mathbf{A}}{m} - \frac{\hat{p}^4}{8m^3c^2}\,, \tag{6.28}$$

one at a time. Considering that we are working with intense fields one should maybe expect the term proportional to $\mathbf{A}^3$ to have a big effect. However, the results showed that this term and the first term of (6.27) did not affect the energy spectrum to any mentionable degree. The second and third term each showed to cause about half of the total displacement seen in figure (6.3). Both these terms are proportional to $\mathbf{A}^2$. It seems that terms proportional to odd powers of $\mathbf{A}$ does not affect the system very much. This might be because they are oscillating with alternating sign and effectively cancel out. Noticing that the LS-coupling also is of an odd power of $\mathbf{A}$:

$$L = \mathbf{r} \times (\mathbf{p} + e\mathbf{A})\,, \tag{6.29}$$

it is reasonable to consider that it would not have caused much alteration of our results had it been implemented in the calculation.

It has been shown by [11, 12, 13, 14, 15, 16] that the dipole approximation breaks down for intense laser fields, and we know that the non-dipole effects in the ionization probability are much greater than the relativistic effects found here. An option for further study could then be to go beyond the dipole approximation and then study the effects of the relativistic interaction terms retaining the space-dependence of the field.

Chapter 7

Summary

The goal of this thesis is twofold: the first objective is to study relativistic effects in photoionization cross section. The second objective is to study relativistic effects in the ionization processes of hydrogen in super-intense laser fields. The results have been obtained by solving both the time independent (TISE) and time dependent Schrödinger equation (TDSE).

To solve the TISE numerically a MATLAB program was written where the starting parameters are: the box size, the truncation of orbital angular momentum quantum number, number of basis functions or eigenvalues and the order of the basis functions. The matrix elements of the Hamiltonian for the TISE has been calculated using this program. The matrix elements were then used as input in a Fortran time propagation program solving the TDSE. The system under study is the hydrogen atom subjected to an intense laser pulse of frequency $\omega = 50$ a.u. with a sine squared envelope pulse with a 15-cycle carrier. The dipole approximation of the field has been applied for all calculations.

The results have been divided into two parts: the time independent photoionization cross section results and the time dependent ionization results. Photoionization cross section for the transitions between $1s$ and kp states have been examined and the results show that the cross section is decreasing with the incoming photon energy. As such, a high energy photon must come closer to the electron for there to be an interaction. A relativistic effect is observed when reaching high photon energies of about 1000 a.u. The total cross section for the relativistic case is lower than for the non-relativistic case and the effect is increasing with increasing photon energy. The relativistic Schrödinger cross section results have been compared to results from calculating the cross section using the Dirac equation [30]. The two different approaches seemed to be in agreement for photon energies up to 1500 a.u. Although we can not conclude this. For photon energies above this value a small deviation can be noticed. In addition, it has been found that the cross section is depending on the total angular momentum quantum number, j. The cross section is generally smaller for $j_- = \frac{1}{2}$ when spin and orbital angular momentum vectors are anti-parallel than for $j_+ = \frac{3}{2}$ when the two vectors are parallel.

Results from solving the time dependent Schrödinger equation with relativistic corrections have been compared to the non-relativistic TDSE and the time dependent Dirac equation. The ionization probability is seen to be lower for the relativistic than for the non-relativistic calculation. This effect is starting to be noticeable at intensities of about $E_0 = 500$ a.u. and it is increasing with electric field strength. This is concurrent with

previous observations solving the Dirac equation [6, 9, 10]. The TDDE and the relativistic TDSE seem to be in agreement. Kinetic energy spectra for the emitted photoelectron at high intensities have been studied as well. Specifically, the case where the electric field strength is $E_0 = 1000$ a.u. which is about $3.5 \cdot 10^{19}$ W/cm. In such a field the electron is expected to reach relativistic velocities. The quiver velocity corresponding to the given electric field strength of $E_0 = 1000$ a.u. and photon frequency of $\omega = 50$ a.u. is $v_{quiv} = 0.15$c. We have compared the results from the relativistic TDSE and the TDDE and found that they are in good agreement. When comparing energy spectra calculated from the relativistic TDSE with non-relativistic TDSE a shift towards higher kinetic energies is observed. The shift is increasing with kinetic energy. It is expected that the shift is caused by the relativistic correction of the electron's momentum [10].

The time propagation has been performed activating only certain terms of the relativistic Hamiltonian at a time. The results show that it is the terms proportional to even powers of the field, $\mathbf{A}^2$, that cause the shift towards higher energies. The terms proportional to odd powers of the field, $\mathbf{A}$ and $\mathbf{A}^3$, do not alter the energy spectrum noticeably and these terms can possibly be neglected in the dipole approximation. A possible reason why these terms do not give any effect might be that they cancel out because they oscillate with alternating sign.

In super-intense fields we know that the dipole approximation breaks down and that beyond dipole effects become important [14, 11, 13, 12, 16]. However, the dipole approximation yields interesting results for the processes studied here, and relativistic effects are clearly noticeable. Suggestions for further work could thus include implementing beyond dipole corrections and study the relativistic effects when retaining the space dependence of the field. Also, a way of implementing the LS-coupling in velocity gauge, which has been neglected in this thesis, would be interesting to explore in order to study the effects of the electric field on the spin-orbit coupling.

Bibliography

[1] J. Gaarder, *Sofies verden : roman om filosofiens historie*. Høst pocket, Høst og søn, 2004.

[2] T. Maiman, *Stimulated Optical Radiation in Ruby*. MacMillan & Company, 1960.

[3] C. I. Moore, A. Ting, S. J. McNaught, J. Qiu, H. R. Burris, and P. Sprangle, "A laser-accelerator injector based on laser ionization and ponderomotive acceleration of electrons," *Phys. Rev. Lett.*, vol. 82, pp. 1688–1691, Feb 1999.

[4] P. Emma, R. Akre, J. Arthur, R. Bionta, C. Bostedt, J. Bozek, A. Brachmann, P. Bucksbaum, R. Coffee, F.-J. Decker, *et al.*, "First lasing and operation of an ångstrom-wavelength free-electron laser," *nature photonics*, vol. 4, no. 9, p. 641, 2010.

[5] H. Yoneda, Y. Inubushi, M. Yabashi, T. Katayama, T. Ishikawa, H. Ohashi, H. Yumoto, K. Yamauchi, H. Mimura, and H. Kitamura, "Saturable absorption of intense hard x-rays in iron," *Nature communications*, vol. 5, p. 5080, 2014.

[6] D. P. Crawford and H. R. Reiss, "Stabilization in relativistic photoionization with circularly polarized light," *Phys. Rev. A*, vol. 50, pp. 1844–1850, Aug 1994.

[7] A. Di Piazza, C. Müller, K. Z. Hatsagortsyan, and C. H. Keitel, "Extremely high-intensity laser interactions with fundamental quantum systems," *Rev. Mod. Phys.*, vol. 84, pp. 1177–1228, Aug 2012.

[8] Y. I. Salamin, S. Hu, K. Z. Hatsagortsyan, and C. H. Keitel, "Relativistic high-power laser–matter interactions," *Physics Reports*, vol. 427, no. 2, pp. 41 – 155, 2006.

[9] L. N. Gaier and C. H. Keitel, "Relativistic classical monte carlo simulations of stabilization of hydrogenlike ions in intense laser pulses," *Phys. Rev. A*, vol. 65, p. 023406, Jan 2002.

[10] T. Kjellsson, S. Selstø, and E. Lindroth, "Relativistic ionization dynamics for a hydrogen atom exposed to superintense xuv laser pulses," *Phys. Rev. A*, vol. 95, p. 043403, Apr 2017.

[11] A. Bugacov, M. Pont, and R. Shakeshaft, "Possibility of breakdown of atomic stabilization in an intense high-frequency field," *Phys. Rev. A*, vol. 48, pp. R4027–R4030, Dec 1993.

[12] N. J. Kylstra, R. A. Worthington, A. Patel, P. L. Knight, J. R. Vázquez de Aldana, and L. Roso, "Breakdown of stabilization of atoms interacting with intense, high-frequency laser pulses," *Phys. Rev. Lett.*, vol. 85, pp. 1835–1838, Aug 2000.

[13] J. R. Vázquez de Aldana, N. J. Kylstra, L. Roso, P. L. Knight, A. Patel, and R. A. Worthington, "Atoms interacting with intense, high-frequency laser pulses: Effect of the magnetic-field component on atomic stabilization," *Phys. Rev. A*, vol. 64, p. 013411, Jun 2001.

[14] M. Gavrila, "Atomic stabilization in superintense laser fields," *Journal of Physics B: Atomic, Molecular and Optical Physics*, vol. 35, no. 18, p. R147, 2002.

[15] M. Førre and A. S. Simonsen, "Nondipole ionization dynamics in atoms induced by intense xuv laser fields," *Phys. Rev. A*, vol. 90, p. 053411, Nov 2014.

[16] T. E. Moe and M. Førre, "Ionization of atomic hydrogen by an intense x-ray laser pulse: An ab initio study of the breakdown of the dipole approximation," *Phys. Rev. A*, vol. 97, p. 013415, Jan 2018.

[17] F. Bloch, "Heisenberg and the early days of quantum mechanics," *Physics Today*, vol. 29, no. 12, pp. 23–27, 1976.

[18] P. W. Atkins and R. S. Friedman, *Molecular quantum mechanics*. Oxford university press, 2011.

[19] D. Griffiths, *Introduction to Quantum Mechanics*. Pearson international edition, Pearson Prentice Hall, 2005.

[20] P. Hemmer, *Kvantemekanikk: P.C. Hemmer*. Tapir akademisk forlag, 2005.

[21] B. Bransden and C. Joachain, *Physics of Atoms and Molecules*. Pearson Education, Prentice Hall, 2003.

[22] D. Griffiths, *Introduction to Electrodynamics*. Cambridge University Press, 2017.

[23] C. Maxwell and Forbes, "1. on the description of oval curves, and those having a plurality of foci," *Proceedings of the Royal Society of Edinburgh*, vol. 2, p. 89–91, 1851.

[24] C. Domb, "James Clerk Maxwell," 2018. [Online; accessed 09.04.2018].

[25] T. Holtebekk, "James Clerk Maxwell. I Store norske leksikon," 2014. [Online; accessed 09.04.2018].

[26] F. Mandl and G. Shaw, *Quantum Field Theory*. A Wiley-Interscience publication, John Wiley & Sons, 2010.

[27] C. De Boor, C. De Boor, E.-U. Mathématicien, C. De Boor, and C. De Boor, *A practical guide to splines*, vol. 27. Springer-Verlag New York, 1978.

[28] H. Bachau, E. Cormier, P. Decleva, J. E. Hansen, and F. Martín, "Applications of b -splines in atomic and molecular physics," *Reports on Progress in Physics*, vol. 64, no. 12, p. 1815, 2001.

[29] L. N. Trefethen and D. Bau III, *Numerical linear algebra*, vol. 50. Siam, 1997.

[30] M. Førre. Private Communication, 2018.

[31] M. K. Gordon and L. F. Shampine, "Interpolating numerical solutions of ordinary differential equations," in *Proceedings of the 1974 Annual Conference - Volume 1*, ACM '74, (New York, NY, USA), pp. 46–53, ACM, 1974.

[32] Y.-C. Han and L. B. Madsen, "Comparison between length and velocity gauges in quantum simulations of high-order harmonic generation," *Phys. Rev. A*, vol. 81, p. 063430, Jun 2010.

[33] E. Cormier and P. Lambropoulos, "Optimal gauge and gauge invariance in non-perturbative time-dependent calculation of above-threshold ionization," *Journal of Physics B: Atomic, Molecular and Optical Physics*, vol. 29, no. 9, p. 1667, 1996.

[34] A. Skeidsvoll, "Modeling interactions between hydrogen-like atoms and intense laser pulses with the dirac equation," May 2018.